Air pollution from biomass burning disrupts early adolescent cortical microarchitecture development

Katherine L. Bottenhorn[1,2], Kirthana Sukumaran[1], Rima Habre[1,3], Joel Schwartz[4], Megan M. Herting[1]

[1] Department of Population and Public Health Sciences, University of Southern California, Los Angeles, CA, USA
[2] Department of Psychology, Florida International University, Miami, FL, USA
[3] Spatial Sciences Institute, University of Southern California, Los Angeles, CA, USA
[4] Department of Environmental Health, Harvard T.H. Chan School of Public Health, Boston, MA, USA

Abstract

Exposure to outdoor particulate matter ($PM_{2.5}$) represents a ubiquitous threat to human health and, in particular, the neurotoxic effects of $PM_{2.5}$ from multiple sources may disrupt neurodevelopment. Studies addressing neurodevelopmental implications of PM exposure have been limited by small, geographically-limited samples and largely focus either on macroscale cortical morphology or postmortem histological staining and total PM mass. Here, we leverage residentially-assigned exposure to six, data-driven sources of $PM_{2.5}$ and neuroimaging data from the longitudinal Adolescent Brain Cognitive Development Study (ABCD Study®), collected from 21 different recruitment sites across the United States. To contribute an interpretable and actionable assessment of the role of air pollution in the developing brain, we identified alterations in cortical microstructure development associated with exposure to specific sources of $PM_{2.5}$ using multivariate, partial least squares analyses. Specifically, average annual exposure (i.e., at ages 8-10 years) to $PM_{2.5}$ from biomass burning was related to impaired neurite development across the cortex between 9 and 13 years of age.

Teaser: Pollution from biomass burning is linked to altered neurite density changes across the cortex between ages 9 to 13 as shown by novel neuroimaging markers.

Keywords: air pollution, neurodevelopment, $PM_{2.5}$ sources, restriction spectrum imaging, adolescence

Corresponding Authors: Drs. Katherine L. Bottenhorn and Megan M. Herting, Department of Population and Public Health Sciences, University of Southern California, Los Angeles, CA, USA | Emails: bottenho@usc.edu, herting@usc.edu

Introduction

Outdoor air pollution and, in particular, exposure to fine particulate matter with aerodynamic diameter less than 2.5µm (i.e., $PM_{2.5}$), is among the greatest threats to human health due to its ubiquity and widespread effects (*1–3*). These effects are exacerbated in children (*4*), who have greater respiratory rates, are usually more physically active, and spend more time outdoors than adults, incurring greater dose and greater effect (*5*). In addition to direct neurotoxic effects, $PM_{2.5}$ exposure has been associated with a number of poor behavioral outcomes, including increased depression and suicide risk (*6–8*), anxiety and psychosis (*9*), and poor performance on cognitive assessments (*10–13*), albeit findings are mixed (*14*, *15*). Together, the risk of $PM_{2.5}$ exposure and breadth of potential neurodevelopmental consequences highlight the importance of leveraging novel neuroimaging methods to elucidate neurotoxicant effects of air pollution on the developing human brain. One challenge in this line of research is that $PM_{2.5}$ is a complex mixture of chemical components (e.g., metals, nitrates, sulfates, carbons) arising from sources including anthropogenic human activities (e.g., traffic, industrial fuel burning), natural and meteorological events (e.g., windblown dust, wildfires). The sources and composition of $PM_{2.5}$ vary geographically (*16*) and can have different effects on human health (*17–21*). Untangling the effects of different sources of $PM_{2.5}$ (e.g., via data-driven source apportionment) is important for understanding the effects of outdoor air pollution exposure on human health and neurodevelopment. Source apportionment analyses can help provide insight as to the origins of outdoor $PM_{2.5}$, which may be helpful in designing mitigation strategies and policies to improve air quality. Overall, mapping neurotoxic effects of $PM_{2.5}$ exposure to sources may facilitate a clearer picture of its neurodevelopmental impacts and provide actionable insights for both parents and policymakers.

In addition to increased exposure, children are likely more susceptible to longer-term effects of $PM_{2.5}$ exposure when it affects their ongoing development. Brain development, in particular, follows a protracted course and continues into the third decade of life (*22–24*). The protracted course of brain maturation (Figure 1A) presents a large window of opportunity for air pollution and $PM_{2.5}$ more specifically to impact neurodevelopment (*25*, *26*). Notably, neurotoxic effects of $PM_{2.5}$ are thought to include ongoing cellular processes throughout childhood and early adolescence, including apoptosis (*27*), changes in dendritic spine density and arborization (*28*, *29*), neurogenesis (*30*), and microglial functioning (*1–3*, *28*). Thus, it is crucial to consider not only individual differences in brain structure and function, but how developmental *changes* relate to different sources of $PM_{2.5}$ exposure, to more fully understand its neurodevelopmental effects. In this realm, most research to date has linked $PM_{2.5}$ exposure to cross-sectional differences in cortical morphology, white matter microarchitecture, and subcortical microarchitecture. Urban air pollution, which includes $PM_{2.5}$, exposure has been associated with increased white matter hyperintensities (*31*, *32*), neurovascular dysfunction and ultrafine particle deposition in the brain (*32*, *33*), metabolic alterations (*34*), and altered white matter microarchitecture in children (*35–37*). Smaller cortical thickness and subcortical volume have been associated with greater exposure to ambient $PM_{2.5}$, as well (*26*, *38–40*). While exposure to $PM_{2.5}$ has documented neurotoxic effects and there is substantial evidence of differential health effects between sources of $PM_{2.5}$, little research has considered source-specific impacts on the brain. Thus, there is a substantial knowledge gap in the literature regarding impacts of $PM_{2.5}$ exposure on cortical microarchitecture, especially with respect to ongoing developmental change and influences of different $PM_{2.5}$ sources.

Fine PM, or $PM_{2.5}$, is small enough to cross the blood brain barrier and, as previously mentioned, induces various cellular processes including neuroinflammation, apoptosis, altered dendritic spine density and arborization, and neurogenesis. Thus, it is feasible that exposure during development may not only impact cortical morphology, but microstructural properties of gray matter tissue. Given what we know about the cellular impacts of PM in the brain, assessing gray matter microarchitecture could provide important neurobiological insight into impacts of PM exposure. Two studies to date have linked $PM_{2.5}$ exposure to subcortical gray matter microarchitecture using diffusion-weighted magnetic resonance imaging (dMRI) approaches, revealing differences in the thalamus, brainstem, nucleus accumbens, and caudate nucleus (*40*, *41*). Animal studies have shown effects of $PM_{2.5}$ exposure

on brain microarchitecture and neuroimaging has linked $PM_{2.5}$ exposure to differences in human subcortical and white matter microarchitecture, but little is known about its effects on human *cortical* microarchitecture. Novel measures from multi-compartment, biophysical dMRI models can provide more detailed estimates of $PM_{2.5}$ effects on cortical gray matter microarchitecture. Specifically, restriction spectrum imaging (RSI) takes advantage of multi-shell diffusion MRI data to separately model diffusion in intracellular and extracellular compartments (*42*). Within intracellular diffusion are anisotropic and isotropic components, that separately estimate cylindrical diffusion, along a primary axis or axes, and spherical diffusion, respectively. Further, histological validation has shown that intracellular RSI measures can provide estimates of cortical neurite (i.e., axon and dendrite) architecture and cellularity (*42*), and may be sensitive to neurobiological processes underlying development during late childhood and early adolescence (e.g., synaptic pruning, apoptosis) (*43*). During early adolescence, neurite density, as indexed by anisotropic intracellular diffusion, is largely decreasing across the cortex, while cellularity, as indexed by isotropic intracellular diffusion, is largely increasing (*44*) (Figure 1B). *In vivo* modeling of gray matter microarchitecture could provide a mechanistic perspective on $PM_{2.5}$ neurotoxicity in the developing brain. As the protracted nature of cortical development creates the largest window of vulnerability to lasting neurotoxic effects of air pollution across the brain, such a perspective could provide important information regarding the translation of childhood exposure into lasting damage to brain and mental health.

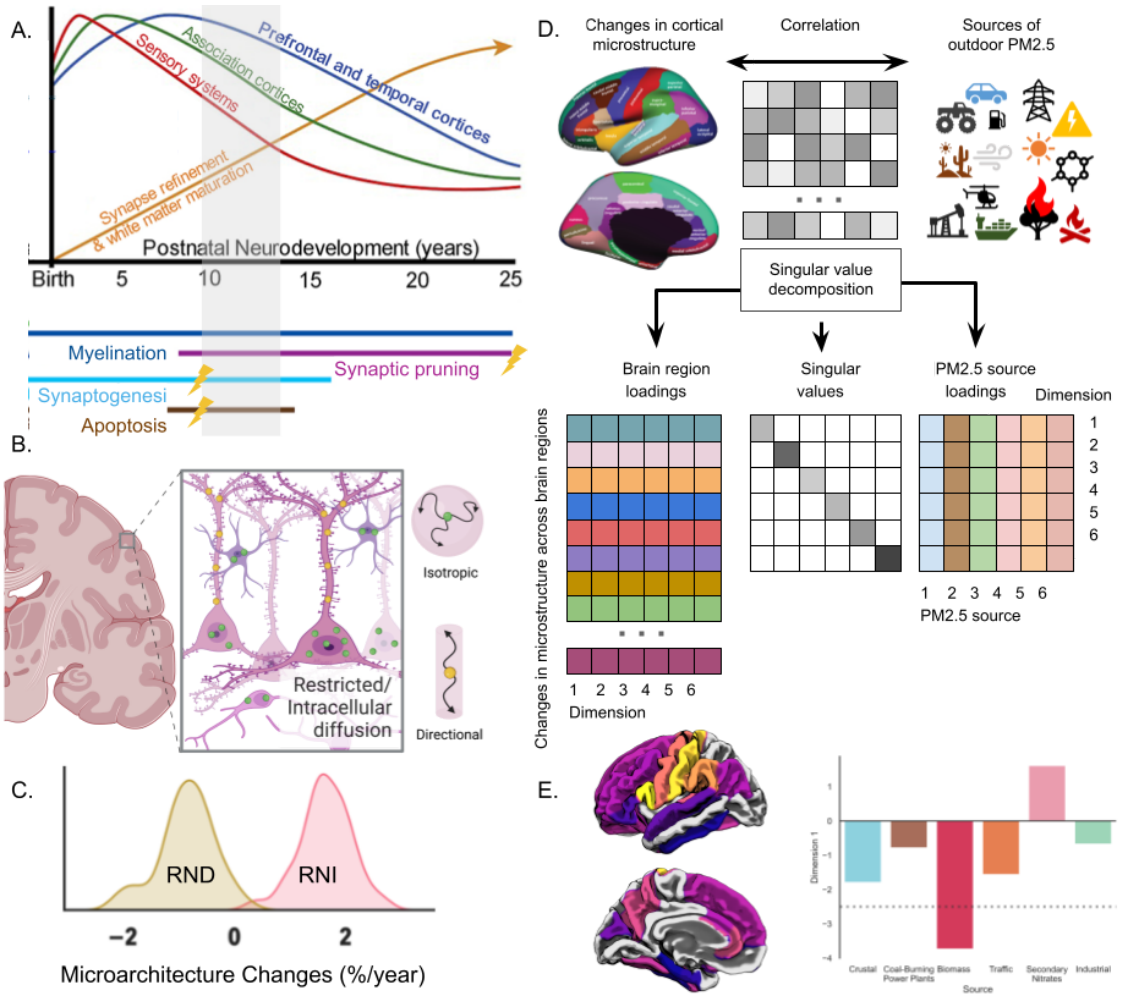

Figure 1. Neurodevelopmental processes and potential impacts of outdoor $PM_{2.5}$ exposure.

Here, we assess source-specific impacts of average annual $PM_{2.5}$ exposure on cortical microarchitecture changes in children between ages 9-10 years and two-years later from the longitudinal, nationwide Adolescent Brain

Cognitive Development Study (ABCD Study®). The ABCD Study enrolled 11,881 children from 21 data collection sites across the United States and includes estimates of 15 chemical components of $PM_{2.5}$ linked to their residential addresses, with $50m^2$ resolution in urban areas and $1km^2$ resolution elsewhere. From these components, we used positive matrix factorization to identify six sources of $PM_{2.5}$ (Sukumaran et al,. in preparation). We chose to assess how one-year average exposure to $PM_{2.5}$ sources during childhood (i.e., between ages 8 and 10 years) were related to changes in cortical microarchitecture between ages 9 and 13 years. Cortical microstructure was estimated from both anisotropic and isotropic intracellular diffusion, reflecting neurite density and cellularity, respectively (*43*, *45–48*), as hypothesized neurotoxic effects of $PM_{2.5}$ likely include disruption to ongoing synaptic refinement during adolescence and altered cellularity due to neuron death and/or reactive gliosis. Using Partial Least Squares Correlation (PLSC), we jointly modeled latent associations between source-specific exposure to $PM_{2.5}$ and changes in cortical microarchitecture (Figure 1D). By investigating source-specific effects on these aspects of early adolescent neurodevelopment (Figure 1E), this work aims to illuminate a more mechanistic and policy-relevant understanding of the developmental neurotoxicity of outdoor air pollution.

Methods

Participants

Longitudinal data were collected as a part of the ongoing Adolescent Brain and Cognitive Development (ABCD) Study, and included in the annual 4.0 and 5.0 data releases (http://dx.doi.org/10.15154/1523041; https://dx.doi.org/10.15154/8873-zj65; Supplementary Table 0). The ABCD Study enrolled 11,881 children 9 to 10 years of age (mean age = 9.49; 48% female) in a 10-year longitudinal study. Participants were recruited at 21 study sites across the United States from elementary schools (private, public, and charter schools) in a sampling design that aimed to represent the nationwide sociodemographic diversity (*49*)**.** All experimental and consent procedures were approved by the institutional review board and human research protections programs at the University of California San Diego. Each participant provided written assent to participate in the study and their legal guardian provided written agreement to participate. For more information, see Garavan et al. (*49*) and Volkow et al. (*50*). Here, we use a subset of data from the ABCD Study, including magnetic resonance imaging (MRI), in addition to measures of participants' sex at birth, socio-demographics, and air pollution exposure. Neuroimaging data include assessments from two time points: baseline enrollment and year 2 follow-up. Sociodemographic and exposure data include assessments from the baseline time point. Exclusion criteria for the ABCD study included lack of English proficiency, severe sensory, neurological, medical or intellectual limitations, and inability to complete an MRI scan (*49*). For this study, we further excluded participants whose 2-year follow-up visit occurred after shutdowns associated with the novel coronavirus pandemic (i.e., March 2020). Shutdowns in response to the COVID-19 pandemic dramatically changed the air quality across the United States due to reductions in commuting, manufacturing, shipping, etc., while also disrupting the lives of youth. Imaging data was excluded if it had incidental neurological findings evident in their scans, failed the ABCD imaging or FreeSurfer quality control procedures (*51*), and/or was missing diffusion-weighted imaging data from either baseline or 2-year follow-up time point.

Demographic Data, Confounders, & Precision Variables

In terms of age, sex, and household size, the ABCD Study cohort closely matches the distribution of 9- and 10-year-olds in the American Community Survey (ACS), a large probability sample survey of U.S. households conducted annually by the U.S. Bureau of Census. The racial breakdown matches closely, too, although children of Asian, American Indian/Alaska Native and Native Hawaiian/Pacific Islander ancestry are under-represented in ABCD (*52*). Confounders and precision variables to be adjusted for in our analyses were identified using a directed acyclic graph (DAG; Supplementary Figure 1) constructed with theoretical knowledge of variables associated with brain development and air pollution exposure. From this DAG, a minimally sufficient set of

covariates were identified, which represent the smallest group of variables that can account for all paths by which the entire variable set may impact air pollution exposure based on the primary residential address and cortical microarchitecture development. Variables included the child's age at baseline data collection (months), sex assigned at birth (*male* or *female*), caregiver-reported race/ethnicity (*White, Black, Hispanic, Asian,* or *Other*), and handedness (*right, left,* or *mixed*; (*53*, *54*)), average daily screen time (hours; (*55*, *56*)), physical activity (number of days child was physically active in the week prior; (*57*)), combined household income in USD (*>100K, 50-100K, <50K,* or *Don't Know/Refuse to Answer*), caregiver-reported perceived neighborhood safety based on a survey modified from PhenX (NSC) (*58*, *59*), and the following information about the child's primary residence: the population density (*60*, *61*), urbanicity (*US Census Track Urban Classification*), distance to major roadways (meters) (*60*), and nighttime noise (i.e., average noise between the hours of 10:00 PM and 7:00 AM in decibels) (*62*). The manufacturer of the MRI on which each participant's data were collected and the average head motion (framewise displacement, mm) throughout diffusion scans at each time point were included in the minimally sufficient set, as well.

Neuroimaging Data

MRI: Acquisition, Processing, and Quality Control

A harmonized data protocol was utilized across sites with either a Siemens, Phillips, or GE 3T MRI scanner. Motion compliance training, as well as real-time, prospective motion correction was used to reduce motion distortion (*63*). T1w images were acquired using a magnetization-prepared rapid acquisition gradient echo (MPRAGE) sequence and T2w images were obtained with a fast spin echo sequence with variable flip angle (*63*). Both consist of 176 slices with $1mm^3$ isotropic resolution. For more details on the scanning protocol, please see Casey et al. (*63*). The DWI acquisition included a voxel size of 1.7 mm isotropic and implements multiband EPI (Moeller et al., 2010; Setsompop et al., 2012) with slice acceleration factor 3. Each DWI acquisition included a fieldmap scan for B0 distortion correction. ABCD employs a multi-shell diffusion acquisition protocol that includes 7 b=0 frames as well as 96 total diffusion directions at 4 b-values (6 with $b = 500\,s/mm^2$, 15 with $b = 1000\,s/mm^2$, 15 with $b = 2000\,s/mm^2$, and 60 with $b = 3000\,s/mm^2$). All images underwent distortion correction, bias field correction, motion correction, and manual and automated quality control per the steps detailed by Hagler and colleagues (2019). After preprocessing, white matter tracts were located and labeled according to the probabilistic atlas AtlasTrack (Hagler et al., 2009). Only images without clinically significant incidental findings (*mrif_score* = 1 or 2) that passed all ABCD Study quality-control parameters were included in analysis (*imgincl_dmri_include* = 1). For a more detailed description of diffusion data processing, please refer to recent work by Gorham & Barch and Hagler et al. (*51*, *64*) and previous papers from our group using these data (*36*, *41*).

Restriction Spectrum Imaging (RSI)

Restriction spectrum imaging (RSI) is an advanced modeling technique that utilizes all 96 directions collected as part of the ABCD Study's multi-shell, high angular resolution imaging (HARDI) acquisition protocol. RSI provides detailed information regarding both the extracellular and intracellular compartments of white matter within the brain (*42*, *65*, *66*). RSI model outputs include normalized measures of intracellular (i.e., restricted), extracellular (i.e., hindered), and free water movement (Figure 1B), all of which are on a unitless scale of 0 to 1. Restricted normalized isotropic signal fraction (RNI), or *isotropic intracellular diffusion,* measures directionless water movement at short distances such that a higher RNI could indicate an increase in number of neuronal cell bodies (i.e., neurogenesis) and/or support cells or swelling of support cells, such as activated astrocytes or microglia as in neuroinflammation (*43*). Restricted normalized directional signal fraction (RND), or *anisotropic intracellular diffusion,* measures directional water movement at short distances and likely indicates intra-neurite (i.e., axons and dendrites) diffusion, with higher RND indicating more myelination, axonal packing, and/or dendritic arborization (*43*). Mean RSI measures are calculated for all cortical ROIs from the Desikan-Killiany atlas

(*67*) to provide estimates of cortical microarchitecture across the brain. As previously published in greater detail, annualized percent change between baseline and 2-year follow up data collection time points was calculated to capture intra-individual changes in cortical microarchitecture (*44*).

Particulate Matter Components and Source Groups

The estimates of outdoor $PM_{2.5}$ exposure represent averages over the initial year of ABCD Study data collection (i.e., 2016) and were compiled and linked based on participants' residential addresses by the ABCD Study's LED workgroup (*60*). At participants' initial study visit, between October 2016 and October 2018, each participant's caregiver reported their primary residential addresses, which were later geocoded to estimate environmental exposures, among other variables. Daily outdoor $PM_{2.5}$ exposure was estimated in $\mu g/m^3$ at $1km^2$ resolution via novel, hybrid, machine-learning based, spatiotemporal models that leverage satellite-based aerosol optical depth observations, along with land-use regression and chemical transport model outputs (*68*, *69*). These daily exposures were, then, averaged over the first year of baseline data collection (2016) to estimate average annual exposure. The ensemble models used to predict annual exposures included neural networks, random forest, and gradient boosting algorithms and were cross-validated with EPA measurements across the U.S., demonstrating excellent performance (spatial R^2 = 0.89, spatial RMSE = $1.26\mu g/m^3$, temporal R^2 = 0.85) (*68*). A similar method was used to estimate 15 separate $PM_{2.5}$ components across the U.S. at a $(50m)^2$ spatial resolution: elemental carbon (EC), organic carbon (OC), silicon (Si), potassium (K), calcium (Ca), bromine (Br), nitrate (NO_3^-), ammonium (NH_4^+), sulfate (SO_4^{2-}), vanadium (V), iron (Fe), nickel (Ni), copper (Cu), zinc (Zn), and lead (Pb). In estimating each component, 166 predictors were used, including temporal and geographical information, observations from satellite (e.g., aerosol optical depth, nighttime lights, vegetation, water index) and meteorological data (e.g., humidity, temperature, wind), emission sources or surrogates thereof (e.g., distance to power plants and highways, traffic counts) (*70*, *71*). For model performance per component, see Supplementary Table 2. As part of a larger scope of ongoing work, we performed source apportionment on these annual estimates of $PM_{2.5}$ components via positive matrix factorization (PMF) using the PMF tool developed and released by United States Environmental Protection Agency (EPA, v5.0) (Sukumaran et al., In preparation). Briefly, PMF decomposes the aforementioned 15 $PM_{2.5}$ components into a predetermined number of sources (or factors), while constraining both the factors and components' contributions to each factor to non-significantly negative (i.e. positive) values. When repeated across a range of potential solutions, evaluating model performance with four to eight samples based on prior source apportionment literature, PMF identified an optimal solution with 6 factors, or sources, corresponding with crustal materials (i.e., soil, dust; Factor 1: V, Si, Ca load highest), secondary ammonium sulfates (Factor 2: SO_4^{2-}, NH_4^+, V), biomass burning (Factor 3: Br, K, OC), traffic emissions (Factor 4: Fe, Cu, EC), secondary ammonium nitrates (Factor 5: NH_4^+, NO_3^-, SO_4^{2-}), and metals potentially from industrial and residential fuel burning (Factor 6: Pb, Zn, Ni, Cu) (Supplementary Figure 2).

Analyses

A data analysis plan was registered with the Open Science Framework (OSF). Here, we used our previously published Partial Least Squares Correlation (PLSC; (*41*)) approach to study latent associations between exposure to $PM_{2.5}$ sources and cortical microarchitecture.

After excluding individuals based on these criteria and the aforementioned MRI quality control criteria, the complete-case sample size for all analyses presented here was 4103 individuals (7334 individuals' 2-year follow-up visit was prior to March 2020, 6230 individuals' baseline and 2-year follow-up dMRI data were of sufficient quality). Descriptive statistics were computed across the final dataset (Table 1), including mean and standard deviation for all continuous variables (i.e., age, screen time, physical activity, perceived neighborhood safety, population density, distance to major roadways, nighttime noise, exposure estimates, changes in

intracellular diffusion, and head motion); mode, and distribution of all categorical variables (i.e., sex assigned at birth, race and ethnicity, handedness, household income, urbanicity).

Prior to performing PSLC, the aforementioned minimally sufficient set of covariates identified from the aforementioned DAG was regressed out of both $PM_{2.5}$ source estimates and annualized percent changes in cortical microarchitecture using a linear model implemented in R (v4.2.0). This model included participant age, sex, handedness, race/ethnicity, average physical activity, average weekday and weekend screen time, in addition to data collection site, MRI manufacturer, average head motion during the dMRI scan, household income and their residential address's proximity to major roadways, urbanicity, area population density, and average nighttime noise level. All following analyses were performed on the residuals from these regressions.

Then, we used PLSC to identify latent associations between $PM_{2.5}$ sources and estimates of cortical gray matter intracellular diffusion. To complement and potentially contextualize the PMF-derived $PM_{2.5}$ sources, we also ran PLSC models for each isotropic and anisotropic intracellular diffusion changes with all 15 of the individual chemical components of PM. Thus, four PLSC models were run: six $PM_{2.5}$ sources and anisotropic intracellular diffusion, six $PM_{2.5}$ sources and isotropic intracellular diffusion, 15 $PM_{2.5}$ components and anisotropic intracellular diffusion, and 15 $PM_{2.5}$ components and isotropic intracellular diffusion.

Briefly, PLSC is a multivariate, cross-decomposition technique that projects multidimensional variable blocks (here: changes in intracellular diffusion, sources of PM) into a lower dimensional subspace such that the covariance between variable blocks is maximized. This process identifies "latent dimensions" of correspondence between blocks by calculating their best fit correlation, constrained to the maximal covariance structure (*72*, *73*). Because PLSC requires complete case data, we used listwise deletion to remove incomplete cases. Here, we used `TExPosition` to perform PLSC (*74*), `Boot4PLSC()` from `data4PCCAR` for bootstrapping to identify significant latent associations (*75*). Versions of all packages used in these analyses are noted in Supplementary Methods.

Prior to running PLSC, $PM_{2.5}$ sources and cortical microarchitecture measures were mean-centered and normalized (to standard deviation of 1). For each block of variables (cortical microarchitecture changes, sources of PM), the residualized, normalized values were arranged into participant-by-variable matrices. For $PM_{2.5}$ sources, this comprised a row per participant and a column per source. For cortical microarchitecture changes, this comprised a row per participant and a column per cortical region. The correlation between these two matrices was then decomposed using singular value decomposition (SVD) into three matrices: a square singular value matrix and a matrix each for $PM_{2.5}$ source and cortical microarchitecture loadings on each latent dimension. Thus, each latent dimension consists of one variable per block of data that was derived from a linear combination of the original variable blocks (i.e., cortical microarchitecture changes, sources of PM) and represents the loading of that block on the latent dimension. These variable loadings, or "saliences", describe how the original variables in each block load contribute to each latent dimension, while the singular values explain the correlation of latent variable pairs, per dimension. An effect size was then calculated per latent dimension, denoting the proportion of covariance between blocks that it explains, from the ratio of that latent dimension's squared singular values to the sum of all latent dimensions' singular values.

We, then, used permutation testing and bootstrapping to assess statistical significance of the overall model and of each latent dimension, respectively (*72*, *73*, *76*). In order to test for statistical significance of the overall model, we used the procedure described by McIntosh and Lobaugh (*73*), in which variables were reordered across 1000 permutations and the probability of the observed solution was computed as the number of times the permuted singular values exceeded the observed singular values. The SVD used in PLSC gives a fixed number of solutions, the upper bound of which is restricted by the number of variables in the smaller block (in this case, 6 solutions due to 6 sources of air pollution). In order to test for statistical significance of variable loadings on each significant observed latent dimension, we used the procedure described by McIntosh and Lobaugh (*73*) and calculated variable loadings from 10,000 bootstrapped samples. These loadings were used to calculate a confidence

bootstrap ratio, which approximates a z-score, per variable per significant latent dimension and determined variables with bootstrap ratios greater than 2.5 (i.e., $p < 0.01$) to significantly load on that dimension. This entire process was performed separately for isotropic and anisotropic intracellular diffusion.

Finally, loadings for changes in cortical microarchitecture and sources of air pollution were plotted against each other to visualize the nature of the relationship. Similarly, the neuroanatomy of each latent association between cortical microarchitecture development and $PM_{2.5}$ source was visualized via cortical surface plots.

Results

The final sample characteristics for the current study are described in Table 1 and average $PM_{2.5}$ component exposures, across participants, are described in Supplementary Table 2. Per-site average participant loadings for each source and average $PM_{2.5}$ component masses are available in Supplementary Table 3 and 4, respectively. Average changes in microarchitecture across the brain in the ABCD Study sample are described elsewhere by Bottenhorn et al. (*44*).

By assessing latent dimensions of association between $PM_{2.5}$ sources and cortical microarchitecture using Partial Least Squares Correlation (PLSC), we revealed a widespread pattern of changes in anisotropic intracellular diffusion related to exposure to $PM_{2.5}$ ($p_{omnibus} < 0.01$; Supplementary Table 5), but no significant association between changes in isotropic intracellular diffusion and other $PM_{2.5}$ sources ($p_{omnibus} = 0.527$; Supplementary Table 5). Latent associations between all 15 chemical components of $PM_{2.5}$ and cortical microarchitecture revealed multiple significant patterns of exposure-related change in both anisotropic and isotropic intracellular diffusion (both $p_{omniobus} < 0.01$; Supplementary Table 5).

Table 1. Sample demographics, compared to those of the full ABCD Study.

	Full ABCD Study		Final Sample*	
	N	%	*N*	%
Total N	11881		4103	34.5%
Age at baseline (months)	118.97 ± 7.50		119.26 ± 7.45	
Missing	41	<1%	0	0%
Sex (F)	5658	48%	1943	47%
Missing	41	<1%	0	0%
Handedness (R)	9398	79%	3287	80%
Race & Ethnicity				
Asian + Other	1493	13%	450	11%
Hispanic	2405	20%	766	19%
Black	1777	15%	405	10%
White	6163	52%	2482	60%
Missing	43	<1%	0	0%
Household Income				
< $50,000	3215	27%	1735	42%
$50,000 to $100,000	3066	26%	1921	47%
> $100,000	4544	38%	2683	65%

Table 1. Sample demographics, compared to those of the full ABCD Study.

	Full ABCD Study		Final Sample*	
	N	%	*N*	%
Didn't know or refused	1013	9%	519	13%
Missing	0	0%	0	0%
Urbanicity				
Urbanized area	9821	83%	3578	87%
Urban cluster	372	3%	157	4%
Rural area	966	8%	368	9%
Missing	722	6%	0	0%
MRI Scanner Manufacturer				
Siemens	7303	61%	2720	66%
GE Medical Systems	2941	25%	942	23%
Philips Medical Systems	1521	13%	441	11%
Missing	116	1%	0	0%
	Mean ± Standard deviation		Mean ± Standard deviation	
Screen Time (weekday; hours)	3.46 ± 3.10		3.11 ± 2.77	
Screen Time (weekend; hours)	4.62 ± 3.63		4.29 ± 3.32	
Physical Activity (days)	3.49 ± 2.32		3.64 ± 2.29	
Neighborhood Safety	3.89 ± 0.98		3.97 ± 0.91	
Population Density	2136.40 ± 2219.72		2023.30 ± 2210.08	
Distance to Roadways (meters)	1187.58 ± 1282.81		1218.05 ± 1399.17	
Nighttime Noise (dB)	51.10 ± 3,91		50.69 ± 3.91	
$PM_{2.5}$ (μg/m^3)	7.52 ± 2.56		7.36 ± 2.54	
Head Motion (mm)	1.31 ± 0.43		1.19 ± 0.19	

Note. *Some missing demographic values in the complete-case sample because "complete" was defined as no missing values for variables of interest (i.e., $PM_{2.5}$ sources, dMRI data) or covariates (i.e., minimally sufficient set, as described in *Demographic Data, Covariates, & Precision Variables*).

Air pollution from biomass burning affects nuanced changes in neurite density during the transition to adolescence

Latent associations between annualized changes in anisotropic intracellular diffusion (i.e., neurite density) and $PM_{2.5}$ sources identified by PLSC included one significant dimension ($p < 0.01$) that accounted for 68% of shared variance between $PM_{2.5}$ sources and neurite density changes (Supplementary Figure 8, Supplementary Table 5). Exposure to $PM_{2.5}$ from biomass burning ($p < 0.01$; Figure 2A) was associated with neuroanatomically diffuse changes in neurite density, spanning brain systems responsible for language, social processing, sensorimotor functions, and executive functioning, in addition to regions of the three brain networks most often linked to psychopathology (i.e., the default mode, central executive, and salience networks (77)), or "triple network" regions (Figure 2B, C). These exposure-related cortical microarchitecture changes were most evident in frontal

gyri, pre- and postcentral gyri, superior temporal gyri, inferior parietal regions, caudal anterior cingulate gyri, right insula, and left caudal anterior cingulate gyrus (see Table 2 for regional saliences). Recalling that cortical anisotropic intracellular diffusion is predominantly decreasing across this developmental period, these positive exposure-brain associations reflect smaller decreases in neurite density. The remaining latent dimensions were not significant at $p < 0.01$ and accounted for 13% (driven by $PM_{2.5}$ from crustal, biomass, and traffic; $p = 0.433$), 8% (driven by secondary ammonium sulfates; $p = 1$), 6% (driven by secondary ammonium sulfates and nitrates; $p = 1$), 3% (driven by industrial $PM_{2.5}$; $p = 1$), and 3% (driven by traffic, crustal; $p = 1$) of shared variance between $PM_{2.5}$ sources and neurite density changes (Supplementary Table 5). In the first two dimensions, together explaining more than 80% of shared variance, $PM_{2.5}$ from biomass burning showed an opposite association with changes in anisotropic intracellular diffusion to crustal- and traffic-related $PM_{2.5}$.

There were two significant latent dimensions of association between $PM_{2.5}$ components and changes in anisotropic intracellular diffusion (both $p < 0.01$) The first dimension represented latent associations between brain development and exposure to key components that contributed to biomass burning and traffic emissions as identified by PMF (elemental carbon (EC), potassium (K), and organic carbon (OC)), in addition to ammonium (NH_4^+) (Supplementary Figure 9A). These patterns of exposure-related changes in anisotropic intracellular diffusion share much of the same neuroanatomy spanning all major brain systems and again reflect less decreases in neurite density, as identified in our $PM_{2.5}$ source model, (Figure 5B,C). The second dimension represented latent associations between right hemisphere parahippocampal and fusiform gyri development and exposure to bromine (Br) and copper (Cu), with higher exposure related to greater decreases in anisotropic intracellular diffusion over time (Supplementary Figure 10A). The remaining latent dimensions each accounted for <10% of shared variance (see Supplementary Table 5).

Chemical components of air pollution indicate limited, nuanced effects of $PM_{2.5}$ exposure on cortical cellularity

While no $PM_{2.5}$ sources showed significant latent associations with changes to isotropic intracellular diffusion, the $PM_{2.5}$ components PLSC model identified three latent dimensions of exposure-related changes in isotropic intracellular diffusion (all $p < 0.01$; Supplementary Table 5, Supplementary Figure 11), with limited effects across the cortex. Similar to the $PM_{2.5}$ components and anisotropic intracellular diffusion model, the first dimension represented latent associations between exposure to K, OC, and NH_4^+ and brain development (Supplementary Figure 12A). Exposure-related changes in isotropic intracellular diffusion along this first dimension spanned sensorimotor and triple network regions, including the left cuneus, precentral, middle frontal, and pericalcarine gyri; bilateral anterior cingulate gyri; and right superior frontal gyrus and insula (Figure 8B,C). This first dimension's pattern of exposure and outcome may reflect further neurodevelopmental impacts of exposure to $PM_{2.5}$ from biomass burning. The second dimension represented latent associations between brain development and exposure to sulfates (SO_4^{2-}) and vanadium (V), which are associated with secondary particle formation from coal combustion (i.e., secondary ammonium sulfates) and heavy residual fuel oil burning, respectively (Supplementary Figure 13A). Exposure-related changes in isotropic intracellular diffusion along this second dimension were restricted to sensorimotor regions including the right precentral gyrus, bilateral cuneus, and bilateral calcarine gyri (Figure 9B,C). Interestingly, greater exposure to SO_4^{2-} and V was related to greater increases in isotropic intracellular diffusion in cuneus and pericalcarine cortex, but to smaller increases in the prefrontal gyrus. Finally, the third dimension included vanadium (V) (Supplementary Figure 14A) which is related to residual fuel oil burning, with exposure-related changes in isotropic intracellular diffusion in sensorimotor (i.e., superior parietal, lateral occipital, and paracentral gyri), language (right inferior temporal gyrus) and triple network (i.e., bilateral inferior parietal and right posterior cingulate, insula, and precuneus) regions (Supplementary Figure 14B,C). Again, we see different directions of effect, as greater exposure was associated

with greater increases in right insula cellularity, but lesser increases in parietal, occipital, and inferior temporal cellularity. The remaining, non-significant latent dimensions accounted for <10% each (Supplementary Table 5).

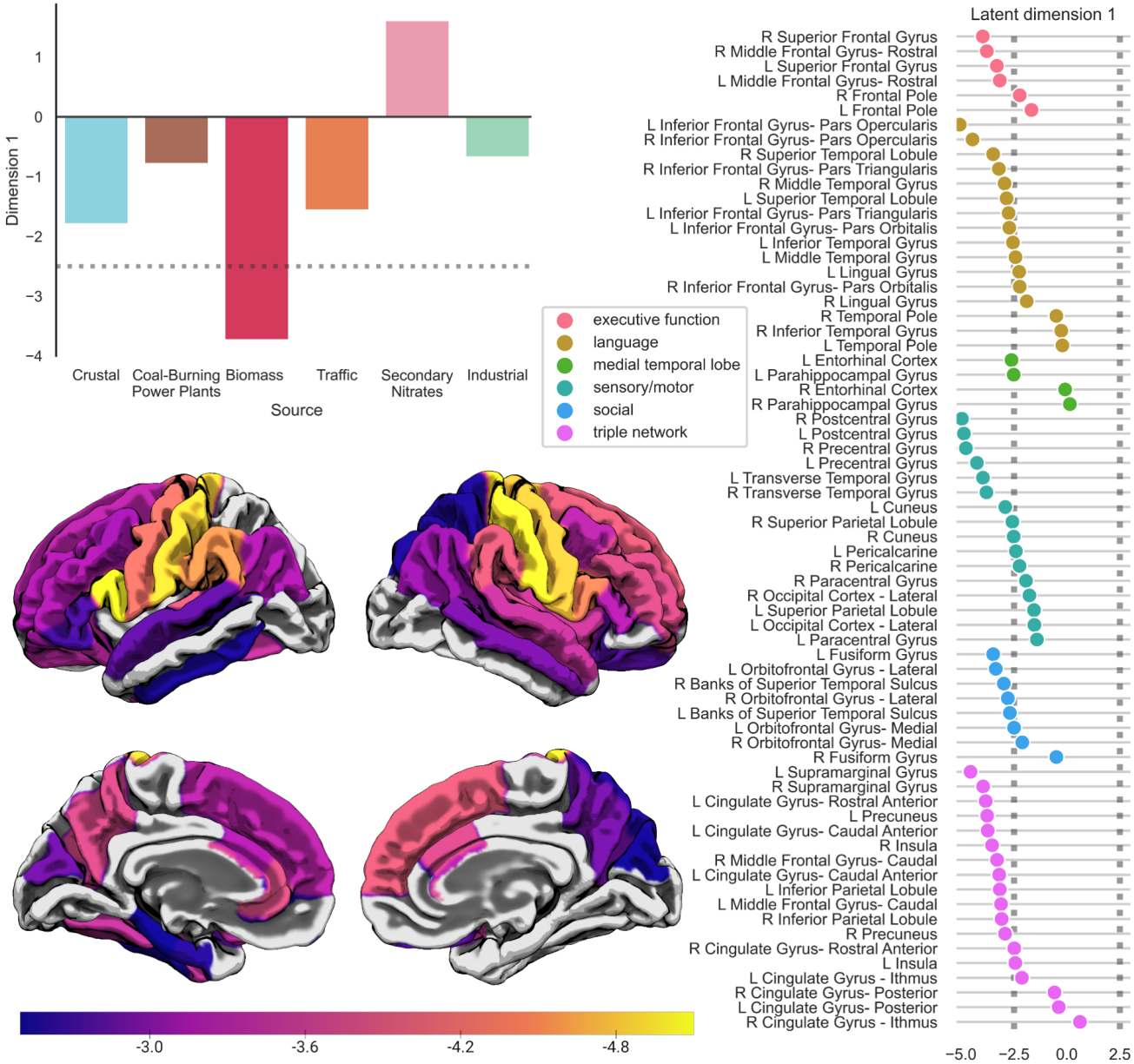

Figure 2. **Changes in cortical neurite density are linked to exposure to pollution from biomass burning.** A. Bootstrap ratios, equivalent to z-scores, indicate significant loadings ($|z| > 2.5$, dashed line) of air pollution from biomass burning on the first latent dimension of brain-pollution associations. B. Bootstrap ratios indicate significant loadings ($|z| > 2.5$; outside the shaded box) of annualized change in anisotropic intracellular diffusion, across brain regions, on the first latent dimension of brain-pollution associations. Loading markers are color-coded based on broad categories of the functions of each brain region. C. Loadings of significant changes in anisotropic intracellular diffusion, by region, on the first latent dimension of brain-pollution association. See Supplementary Table 6 for numerical estimates of brain and pollution saliences.

Discussion

Particulate matter less than 2.5μm in aerodynamic diameter ($PM_{2.5}$) emitted from biomass burning is related to a widespread pattern of cortical microarchitecture development that conflicts with ongoing age-related changes during early adolescence. Cortical anisotropic intracellular diffusion, thought to reflect neurite (i.e., axon and dendrite) density, is largely decreasing during this developmental period (*44*), which may reflect ongoing synaptic pruning and subsequent refinement of neural circuitry that occurs during this developmental period. Greater exposure to $PM_{2.5}$ from biomass burning is linked to smaller decreases in neurite density, which suggests disruption to these ongoing developmental changes. No other source of $PM_{2.5}$ was significantly related to cortical microarchitecture development. However, individual chemical components showed latent associations with microarchitecture development, suggesting that a single source may have differential effects on brain development due to its specific chemical composition mixture, while individual components might have source-independent effects. Developmental changes in isotropic intracellular diffusion, likely reflecting neuronal cell bodies or support cells, was unrelated to source-specific PM exposure; although individual components of biomass burning (i.e., K, OC) and secondary ammonium sulfates (i.e., NH_4^+, SO_4^{2-}, V) were associated with nuanced changes. This work makes important contributions to the literature on the health effects of $PM_{2.5}$ air pollution exposure in several key ways. First, it assesses exposure-related *changes* in the brain, to complement extant cross-sectional neuroimaging studies of brain-exposure associations reviewed in (*38*). Second, it assesses *cortical* microarchitecture, using a multi-compartment biophysical model that is sensitive to differences in cortical cytoarchitecture (White et al., 2013), to complement the existing literature on white matter and subcortical microarchitecture (*36*, *41*, *78*, *79*). Third, it leverages a large, geographically diverse sample and $PM_{2.5}$ source apportionment for more interpretable, actionable insights into the role of specific sources of $PM_{2.5}$ exposure in brain development.

Exposures within federal air quality standards linked to cortical development changes that echo high-exposure neurotoxicity

The majority of *in vivo* studies of differences in the human brain related to air pollution exposure have been limited by cross-sectional neuroimaging data and are, thus, unable to consider ongoing impacts of exposure within an individual. Here, we use estimates of annualized change in cortical microarchitecture between ages 9-10 and 11-13 years to capture broad intra-individual change and inter-individual differences therein (*44*, *80*) during a sensitive period for neurodevelopment (*81*), including microglial-mediated development (*82*). During this age range, anisotropic intracellular diffusion is decreasing across the cortex (*44*), but our current results suggest that individuals with greater exposure to $PM_{2.5}$ components attributable to biomass burning are decreasing less. Anisotropic, or directional, intracellular diffusion reflects water movement within cylindrical intracellular spaces (e.g., axons, dendrites, glial processes). At the resolution of the diffusion-weighted images used here, anisotropic intracellular diffusion would represent aggregated parallel cylindrical intracellular spaces within a voxel (here, 1.7mm isotropic) such as those found in cortical columns and macrocolumns (~350 to 600μm) (*83*). Thus, the data presented here may provide a coarse estimate of the directional organization of cortical macrocolumns, averaged across a gyrus. In the human brain, synaptic pruning follows a protracted course of development, continuing throughout early adolescence, though decreases in neuronal cell bodies occur earlier in development. The process of synaptic refinement likely includes retraction and fragmentation of neuronal and glial processes (*84*). Anisotropic intracellular diffusion, thought to represent neurite density, may be sensitive to this process. If that is the case, then pruning along an axis (e.g., within a cortical column, in which neurons are vertically connected) could manifest as a decrease in anisotropic intracellular diffusion. This notion is supported by links between anisotropic intracellular diffusion and genes that are responsible for neurite morphogenesis (*85*, *86*).

In this constellation of neurobiological associations, we should consider, too, the role of microglia, which are related to intracellular diffusion estimates (*87*). Not only do microglia play an important role in response to

systemic inflammation, recent research highlights their importance in the ongoing synaptic refinement that continues into adolescence (*82*). By incorporating *in vivo* neuroimaging with virtual histology and gene expression data from the Allen Brain Atlas, Vidal-Pineiro et al. found that microglia expression was inversely related to cortical thinning in youth, but positively related to cortical thinning in aging adults (*88*). As cortical thinning is thought to reflect, in part, synaptic pruning, Vidal-Pineiro and colleagues inferred that these contrasting associations reflect a changing role of microglia across the lifespan: from neuronal support in youth to pro-inflammatory immune responses in aging. As our findings suggest a PM-related decrease in adolescent synaptic pruning, evidenced by a positive association between PM and neurite density, is it possible a PM-induced inflammatory response is co-opting the ongoing microglia-mediated synaptic pruning during this period of development?

Pro-inflammatory actions of microglia have been observed *in vitro* following $PM_{2.5}$ exposure (*89*) and implicated in neurodegenerative diseases including Alzheimer's disease (*90*, *91*). This link between microglia functioning in normal development and the pro-inflammatory actions of microglia following $PM_{2.5}$ exposure and in Alzheimer's disease (AD) is important because exposure-related, Alzheimer's-like pathologies have been observed in children as young as 11 months (*92*). Further, marked progression of AD-like pathologies have been documented in adults younger than 30 years old living in Mexico City, with high $PM_{2.5}$ exposure (*93*). These findings are supported by experiments in a mouse model that identified Alzheimer's-like neuroinflammation after as few as 3 months of PM exposure (*94*, *95*), which are followed by cognitive decline after 9 months (*96*). The air pollution levels in this sample are considerably lower than those in Metropolitan Mexico City, but several links between the findings of Calderon-Garciduenas et al. and these findings, in combination with prior work on this data, warrant further investigation. First, early pathologies of air pollution exposure (including $PM_{2.5}$) are seen in the brainstem (*97*, *98*), which displays exposure-related differences in isotropic intracellular diffusion at ages 9-10 years (*41*), suggesting the methods used here may be sensitive to such pathologies. Second, anisotropic *and* isotropic intracellular diffusion are related to both genes and epigenetic related cellular processes underlying synaptic pruning and neuroinflammation (*87*), the dysregulation of which contributes to Alzheimer's pathology (*99*, *100*). Third, early adolescent brain development is characterized by synaptic pruning, but potentially via different cellular mechanisms than in aging and neurodegenerative diseases (*88*). Epidemiological studies have, similarly, found that $PM_{2.5}$ exposure increases risk of Alzheimer's disease (*101*–*104*). Furthermore, some components of $PM_{2.5}$ are related to increased risk of Alzheimer's disease, including black and organic carbon, sulfates, and ammonium (*105*). Thus, the exposure-related disruption of decreasing anisotropic intracellular diffusion seen here may reflect early steps in the neurobiological cascade that leads to premature neurodegenerative pathologies linked to $PM_{2.5}$ exposure.

Experiments in mice suggest that the cortex may have a lower threshold for lasting air pollution-related disruptions than subcortical regions (*106*), evidenced by greater increases in microglia and a larger window of antioxidant system susceptibility in cortex, compared to the striatum. These findings highlight the importance of our current findings, as the neurotoxicity of air pollution is relatively less investigated in the potentially more susceptible cortex. We found largely positive associations between exposure and anisotropic intracellular diffusion changes, revealing that greater exposure is linked to smaller decreases in neurite density. This is further supported by studies demonstrating air pollution-related differences in cortical macrostructure (i.e., cortical thickness, area, and volume) in similarly-aged children consistent with disrupted synaptic pruning (*39*, *107*). More neuroanatomically specific, anisotropic intracellular diffusion is linked to the enrichment of epigenetic markers in the cingulate gyrus (*87*), which is among the regions most impacted by $PM_{2.5}$ exposure seen here and also in rodent models (*108*). Prior work with this data revealed that the anterior cingulate gyrus exhibits largest decreases in anisotropic intracellular diffusion during early adolescence (*44*). Thus, the relatively strong association between exposure to $PM_{2.5}$ from biomass burning and changes to anisotropic intracellular diffusion in the rostral anterior cingulate gyrus may indicate marked regional vulnerability given more dynamic remodeling that occurs during this period of early adolescence.

Source-specific modeling highlights the dangers and neurotoxicity of air pollution from biomass burning

From nationwide modeled annual estimates of 15 $PM_{2.5}$ components, a positive matrix factorization (PMF) analysis identified six overarching sources of $PM_{2.5}$ exposure. Of these, a source loading highly in bromine (Br), potassium (K), and organic carbon (OC) was attributed to biomass burning (Sukumaran et al., forthcoming). Biomass burning comprises smoke from wildfires, wood burning for residential heating and industrial power production, prescribed burns, land clearing, restaurant emissions (especially from meat cooking), and other sources of organic matter combustion (*109–113*). The PMF results reported here are similar to those of Sarnat and colleagues, who applied PMF, chemical mass balance, and tracer methods to study sources of pollution in the Atlanta, GA U.S. metropolitan area from 1998 to 2002; and from 1998 to 2010 (*18*, *21*). They, likewise, identified six sources corresponding with crustal materials, secondary nitrate and sulfate aerosols, traffic, heavy (i.e., industrial) fuel burning, and biomass burning. A recent U.S.-wide source apportionment study using data from 2001 to 2014 with slightly different methods and several additional trace element measurements nonetheless revealed five sources that align with the sources identified here: traffic, soil (i.e., crustal), coal (related to secondary sulfates, nitrates), oil (e.g., industrial), and biomass burning (*114*). In assessing source-specific effects on same-day hospital admissions, biomass burning and secondary organic carbon were consistently among the sources most related to cardiovascular disease, though biomass burning only accounted for 7-8% of total $PM_{2.5}$ (*21*). Similar results were found when assessing links between $PM_{2.5}$ from biomass burning and cardiovascular and respiratory emergency department visits in the United States (*115*, *116*), cardiovascular, natural, and lung cancer mortality, along with systemic inflammation in Europe (*117–119*). In addition to specific cardiorespiratory and inflammatory impacts, combustion, specifically the K and organic carbon produced by biomass burning, are consistently and strongly associated with overall mortality (*120*, *121*). While these associations are on a different temporal scale than the data analyzed here, they align with our current findings linking individual $PM_{2.5}$ components to neurite density changes, which suggests that elemental and organic carbon, potassium, and ammonium drive the source-specific effects observed here. Thus, our findings add to substantial evidence of specific health effects due to exposure to $PM_{2.5}$ from biomass burning, compared with other sources.

PM affects brain health indirectly, via systemic inflammation following inhalation and deposition in the lungs where it may then enter the bloodstream, and possibly directly, by entering the nose and crossing the piriform plate to the olfactory nerve and by traveling along the trigeminal nerve to the brainstem (*122–124*). Further, systemic inflammation increases permeability of the blood-brain barrier, potentially allowing circulating PM to be deposited in the brain. Ultrafine particles (UFPs; <100nm), which are smaller than $PM_{2.5}$ and thus included in $PM_{2.5}$ estimates, have been seen in post mortem brain tissue (*125*), including that of otherwise healthy, young people (*32*, *33*, *126*). Non-human animal studies demonstrate that PM in the brain causes oxidative toxicity, lipid peroxidation, cell death, reactive gliosis, and the release of pro-inflammatory cytokines from microglia (*122*, *123*, *127–131*). Among contributors to $PM_{2.5}$ from biomass burning, wildfire smoke is among the most researched. Wildfire smoke can cause infiltration of peripheral immune cells into the brain, decreases in protective neurometabolites, and increases in pro-inflammatory microglia phenotypes in mice (*129*). However, these responses do differ between brain regions (*128*, *130*, *132*). Furthermore, prior research has shown that wildfire smoke has a particularly high concentration of UFPs and that PM from wildfire smoke causes greater oxidative stress than PM from other sources (*123*). Altogether, cellular and molecular studies of $PM_{2.5}$ impacts on the brain, especially those of a major biomass burning source in wildfire smoke, underscore the patterns of exposure-related microarchitecture changes uncovered here.

Disrupted cortical microarchitecture development coalesce with exposure-related differences in subcortex and white matter at ages 9-10 years

This is the first study of its kind to longitudinally assess *in vivo* disruptions of cortical microarchitecture related to $PM_{2.5}$ air pollution exposure in humans. Our recent work, also based on the ABCD Study cohort, has identified differences in cortical and subcortical gray matter macrostructure (*107*), white matter microarchitecture (*36*) and subcortical gray matter microstructure (*41*) related to total outdoor $PM_{2.5}$ exposure in children ages 9-10 years. Specifically, exposure to outdoor $PM_{2.5}$ was linked to greater isotropic intracellular diffusion in white matter pathways that connect many of the cortical gray matter regions studied here, including the superior longitudinal fasciculus (connecting frontal, angular, and superior parietal gryi), fornix (connecting hippocampus to nucleus accumbens and thalamus), uncinate fasciculus (connecting medial temporal and orbitofrontal cortices), and hippocampal cingulum (innervating the hippocampus and cingulate gyrus) (*36*). Moreover, subcortical isotropic intracellular diffusion in gray matter structures of the accumbens, thalamus, and brainstem were all greater in children with greater $PM_{2.5}$ exposure (*41*). Here, we extend this literature with a novel foray into assessing impacts of sources and $PM_{2.5}$ components of exposure on *cortical changes in* microarchitecture. Notably, we found disrupted developmental change in the cortical regions connected by the aforementioned white matter tracts affected by $PM_{2.5}$ exposure at ages 9-10 years (e.g., cingulate, frontal, angular, and parietal). Although there were no observed hippocampal macro- or microstructure differences linked to specific $PM_{2.5}$ source exposures at ages 9-10 years, the broader picture seems to center largely on regions and tracts connected to the hippocampus and brain regions closely associated with its functions. This is interesting, given the volume of literature in humans and nonhuman animals linking PM exposure to hippocampal inflammation (*133*). Furthermore, hippocampal dysfunction is a hallmark of neurodegenerative disorders (*134*), incidence of which has been linked to air pollution and specifically $PM_{2.5}$ exposure (*92*, *93*, *103*) and the pathologies of which have been observed in children and young adults exposed to high levels of air pollution (*14*, *92*, *93*).

Taken together, disrupted cortical development due to $PM_{2.5}$ exposure may have further implications for adolescent mental health. Adolescence is a time of heightened vulnerability to psychopathology, with peak incidence around 14 years of age (*135*). Abnormal synaptic pruning and exposure to $PM_{2.5}$ have both been linked to increases in mental health problems (*6*, *136*, *137*), along with neurological differences consistent with neurodevelopmental disorders (*138*). Although prior work by our lab and others have found little to no association between total outdoor $PM_{2.5}$ exposure and mental health problems in late childhood and early adolescence (*139*), although these analyses have not been repeated with source-specific exposure estimates. A possible explanation, that unifies the neuroimaging and behavioral findings, is that these differences and changes in brain structure and function associated with $PM_{2.5}$ exposure may act as early signs, or biomarkers, of developing psychopathology later on in adolescence and young adulthood. Thus, the disruptions to cortical microarchitecture development related to biomass burning $PM_{2.5}$ exposure shown here may reflect early, pre-clinical impacts with more serious future implications.

Recommendations for parents and policymakers

While $PM_{2.5}$ levels have largely decreased in recent decades, the contribution from biomass burning has increased and in some regions across the US (*140*, *141*) and wildfires are increasingly responsible for $PM_{2.5}$ levels (*142–145*). Further, human-caused climate change and wildfires have a bidirectional relationship, such that climate change is leading to more and larger fires, which release gasses and PM that amplify climate change (*146*). Thus, exposure to $PM_{2.5}$ from biomass burning is becoming more prevalent even as air quality improves otherwise. While wildfires are not the only source of biomass burning, wildfire smoke crosses state, province, and national borders, affecting individuals beyond the jurisdictions in which they burn. Federal and international monitoring and policy-based mitigation efforts are required to lessen the potential impacts of biomass burning on child and adolescent brain development. The demonstrated neurotoxicity of particles produced by biomass burning and

their serious threats to human health and child brain development underscore the importance of mitigating exposure. The findings presented here suggest that such effects are present in children with exposure below the United States EPA's national standards, before observable detriment to cognition and mental health. Avoiding exposure, especially in children, will require air quality monitoring, staying indoors when air quality is poor, and frequently changing air filters on air conditioning units or using air filtration to assure good indoor air quality.

Limitations

Geographical location plays a role in the sources and composition of $PM_{2.5}$, but is also linked to many other environmental exposures, both directly and indirectly. Local geography, pollution exposure, built and social environments, sociodemographics, and air quality are all intricately linked and can be modeled comprehensively by the "exposome" (*147–149*). Future work will need to apply a comprehensive, "omics" approach to partial out potential roles of the built and social environment in brain development, and how they complicate the exposure-neurodevelopment associations seen here.

Using region-averaged neuroimaging data simplifies interpretability, reduces dimensionality in a neuroanatomically-informed manner, and may increase signal-to-noise ratio, similar to the effects of spatial smoothing in MRI data. However, Palmer et al. demonstrate considerable heterogeneity in cortical, subcortical, and white matter microarchitecture within regions using a voxelwise approach (i.e., not averaged across gyri, regions, or tracts) in the same data. Future research is needed to assess exposure-neurodevelopment associations seen within regions of cortical microarchitecture.

Finally, although the ABCD Study sampling procedures aimed to assemble a sample that is sociodemographically representative of the population of the United States, the final sample over represents youth from wealthier, whiter, and more educated households. The quality control procedures employed here and exclusion of individuals with incomplete data further limit generalizability of these findings. Future studies are warranted that include larger representation of lower income and minoritized backgrounds, which have greater burden to exposure in the U.S. (*150*, *151*).

Conclusions

Here, we identified a pattern of disruptions to early adolescent cortical development linked to exposure to $PM_{2.5}$ air pollution largely attributable to biomass burning. Between ages 9 and 13 years, synaptic pruning is ongoing across the cortex, facilitated in part by the actions of microglia. This process may be reflected by anisotropic intracellular diffusion, reflecting neurite density, decreases seen across the cortex in this age range. The current study shows that individuals with greater exposure show smaller decreases in anisotropic intracellular diffusion over time. Because the intracellular diffusion estimates used here are likely sensitive to changes in neurite density and organization, these findings may link exposure to particulate matter from biomass burning to impaired synaptic pruning. Cellular and histological studies have linked air pollution exposure to pro-inflammatory changes in microglia functioning, which may explain the observed disruptions during adolescence. Policymakers should consider putting greater emphasis on anthropogenic activities that contribute to biomass burning, in order to minimize any long-term harm caused by disrupted cortical development due to $PM_{2.5}$ exposure.

Acknowledgments

A special thank you to all of the children and families for their participation in their ABCD Study.

Research described in this article was supported by the National Institutes of Health (MMH: NIEHS R01ES032295, R01ES031074; KLB: P30ES07048-27) CCI would like to acknowledge scholars involved in NSP (R25 NS089462), BRAINS (R25 NS094094), and Diversifying CNS (R25 NS117356), as well as R25MH125545 and R25MH120869 for creating a supportive network of ABCD Study users.

Data used in the preparation of this article were obtained from the Adolescent Brain Cognitive Development℠ (ABCD) Study (https://abcdstudy.org), held in the NIMH Data Archive (NDA). This is a multisite, longitudinal study designed to recruit more than 10,000 children age 9-10 and follow them over 10 years into early adulthood. The ABCD Study® is supported by the National Institutes of Health and additional federal partners under award numbers U01DA041048, U01DA050989, U01DA051016, U01DA041022, U01DA051018, U01DA051037, U01DA050987, U01DA041174, U01DA041106, U01DA041117, U01DA041028, U01DA041134, U01DA050988, U01DA051039, U01DA041156, U01DA041025, U01DA041120, U01DA051038, U01DA041148, U01DA041093, U01DA041089, U24DA041123, U24DA041147. A full list of supporters is available at https://abcdstudy.org/federal-partners.html. A listing of participating sites and a complete listing of the study investigators can be found at https://abcdstudy.org/consortium_members/. ABCD consortium investigators designed and implemented the study and/or provided data but did not necessarily participate in the analysis or writing of this report. This manuscript reflects the views of the authors and may not reflect the opinions or views of the NIH or ABCD consortium investigators. The ABCD data repository grows and changes over time. The ABCD data used in this report came from http://dx.doi.org/10.15154/1523041.

Competing Interests

The authors declare no competing interests.

Author Contributions

Conceptualization: KLB, MMH
Data curation: KLB, KS, JS?
Formal Analysis: KLB, KS?
Funding acquisition: MMH, KLB?
Methodology: KLB, MMH, RH
Project administration: KLB, MMH
Resources: MMH, JS
Software: KLB, KS
Supervision: MMH
Visualization: KLB
Writing – original draft: KLB, MMH
Writing – review & editing: KLB, KS, RH, JS, MMH

References

1. L. G. Costa, T. B. Cole, J. Coburn, Y.-C. Chang, K. Dao, P. J. Roqué, Neurotoxicity of traffic-related air pollution. *NeuroToxicology* **59**, 133–139 (2017).
2. S. Genc, Z. Zadeoglulari, S. H. Fuss, K. Genc, The Adverse Effects of Air Pollution on the Nervous System. *J. Toxicol.* **2012**, e782462 (2012).
3. C. Cardenas-Iniguez, E. Burnor, M. M. Herting, Neurotoxicants, the Developing Brain, and Mental Health. *Biol. Psychiatry Glob. Open Sci.* **2**, 223–232 (2022).
4. H. L. Brumberg, C. J. Karr, A. Bole, S. Ahdoot, S. J. Balk, A. S. Bernstein, L. G. Byron, P. J. Landrigan, S. M. Marcus, A. L. Nerlinger, S. E. Pacheco, A. D. Woolf, L. Zajac, C. R. Baum, C. C. Campbell, J. A. Sample, A. J. Spanier, L. Trasande, COUNCIL ON ENVIRONMENTAL HEALTH, Ambient Air Pollution: Health Hazards to Children. *Pediatrics* **147**, e2021051484 (2021).
5. T. F. Bateson, J. Schwartz, Children's Response to Air Pollutants. *J. Toxicol. Environ. Health A* **71**, 238–243 (2007).
6. I. Braithwaite, S. Zhang, J. B. Kirkbride, D. P. J. Osborn, J. F. Hayes, Air Pollution (Particulate Matter) Exposure and Associations with Depression, Anxiety, Bipolar, Psychosis and Suicide Risk: A Systematic Review and Meta-Analysis. *Environ. Health Perspect.* **127**, 126002 (2019).
7. S. Heo, W. Lee, M. L. Bell, Suicide and Associations with Air Pollution and Ambient Temperature: A Systematic Review and Meta-Analysis. *Int. J. Environ. Res. Public. Health* **18**, 7699 (2021).
8. Q. Liu, W. Wang, X. Gu, F. Deng, X. Wang, H. Lin, X. Guo, S. Wu, Association between particulate matter air pollution and risk of depression and suicide: a systematic review and meta-analysis. *Environ. Sci. Pollut. Res.* **28**, 9029–9049 (2021).
9. J. B. Newbury, R. Stewart, H. L. Fisher, S. Beevers, D. Dajnak, M. Broadbent, M. Pritchard, N. Shiode, M. Heslin, R. Hammoud, M. Hotopf, S. L. Hatch, I. S. Mudway, I. Bakolis, Association between air pollution exposure and mental health service use among individuals with first presentations of psychotic and mood disorders: retrospective cohort study. *Br. J. Psychiatry* **219**, 678–685 (2021).
10. J. L. Allen, G. Oberdorster, K. Morris-Schaffer, C. Wong, C. Klocke, M. Sobolewski, K. Conrad, M. Mayer-Proschel, D. A. Cory-Slechta, Developmental neurotoxicity of inhaled ambient ultrafine particle air pollution: Parallels with neuropathological and behavioral features of autism and other neurodevelopmental disorders. *NeuroToxicology* **59**, 140–154 (2017).
11. A. Clifford, L. Lang, R. Chen, K. J. Anstey, A. Seaton, Exposure to air pollution and cognitive functioning across the life course – A systematic literature review. *Environ. Res.* **147**, 383–398 (2016).
12. M. Guxens, M. J. Lubczyńska, R. L. Muetzel, A. Dalmau-Bueno, V. W. V. Jaddoe, G. Hoek, A. van der Lugt, F. C. Verhulst, T. White, B. Brunekreef, H. Tiemeier, H. El Marroun, Air Pollution Exposure During Fetal Life, Brain Morphology, and Cognitive Function in School-Age Children. *Biol. Psychiatry* **84**, 295–303 (2018).
13. M. Guxens, R. Garcia-Esteban, L. Giorgis-Allemand, J. Forns, C. Badaloni, F. Ballester, R. Beelen, G. Cesaroni, L. Chatzi, M. de Agostini, A. de Nazelle, M. Eeftens, M. F. Fernandez, A. Fernández-Somoano, F. Forastiere, U. Gehring, A. Ghassabian, B. Heude, V. W. V. Jaddoe, C. Klümper, M. Kogevinas, U. Krämer, B. Larroque, A. Lertxundi, N. Lertxuni, M. Murcia, V. Navel, M. Nieuwenhuijsen, D. Porta, R. Ramos, T. Roumeliotaki, R. Slama, M. Sørensen, E. G. Stephanou, D. Sugiri, A. Tardón, H. Tiemeier, C. M. T. Tiesler, F. C. Verhulst, T. Vrijkotte, M. Wilhelm, B. Brunekreef, G. Pershagen, J. Sunyer, Air Pollution During Pregnancy and Childhood Cognitive and Psychomotor Development: Six European Birth Cohorts. *Epidemiology* **25**, 636–647 (2014).
14. E. Essers, A.-C. Binter, A. Neumann, T. White, S. Alemany, M. Guxens, Air pollution exposure during pregnancy and childhood, APOE ε4 status and Alzheimer polygenic risk score, and brain structural morphology in preadolescents. *Environ. Res.* **216**, 114595 (2023).
15. M. S. W. Kusters, E. Essers, R. Muetzel, A. Ambrós, H. Tiemeier, M. Guxens, Air pollution exposure during pregnancy and childhood, cognitive function, and emotional and behavioral problems in adolescents. *Environ. Res.* **214**, 113891 (2022).
16. G. Snider, C. L. Weagle, K. K. Murdymootoo, A. Ring, Y. Ritchie, E. Stone, A. Walsh, C. Akoshile, N. X. Anh, R. Balasubramanian, Variation in global chemical composition of PM 2.5: emerging results from SPARTAN. *Atmospheric Chem. Phys.* **16**, 9629–9653 (2016).
17. C. Chen, J. A. Warrington, F. Dominici, R. D. Peng, D. C. Esty, J. F. Bobb, M. L. Bell, Temporal variation in association between short-term exposure to fine particulate matter and hospitalisations in older adults in

the USA: a long-term time-series analysis of the US Medicare dataset. *Lancet Planet. Health* **5**, e534–e541 (2021).
18. Y. Chung, F. Dominici, Y. Wang, B. A. Coull, M. L. Bell, Associations between Long-Term Exposure to Chemical Constituents of Fine Particulate Matter (PM2.5) and Mortality in Medicare Enrollees in the Eastern United States. *Environ. Health Perspect.* **123**, 467–474 (2015).
19. F. Holguin, Traffic, Outdoor Air Pollution, and Asthma. *Immunol. Allergy Clin. North Am.* **28**, 577–588 (2008).
20. F. Kazemiparkouhi, T. Honda, K.-D. Eum, B. Wang, J. Manjourides, H. H. Suh, The impact of Long-Term PM2.5 constituents and their sources on specific causes of death in a US Medicare cohort. *Environ. Int.* **159**, 106988 (2022).
21. J. A. Sarnat, A. Marmur, M. Klein, E. Kim, A. G. Russell, S. E. Sarnat, J. A. Mulholland, P. K. Hopke, P. E. Tolbert, Fine Particle Sources and Cardiorespiratory Morbidity: An Application of Chemical Mass Balance and Factor Analytical Source-Apportionment Methods. *Environ. Health Perspect.* **116**, 459–466 (2008).
22. M. M. Herting, R. Kim, K. A. Uban, E. Kan, A. Binley, E. R. Sowell, Longitudinal changes in pubertal maturation and white matter microstructure. *Psychoneuroendocrinology* **81**, 70–79 (2017).
23. M. M. Herting, C. Johnson, K. L. Mills, N. Vijayakumar, M. Dennison, C. Liu, A.-L. Goddings, R. E. Dahl, E. R. Sowell, S. Whittle, N. B. Allen, C. K. Tamnes, Development of subcortical volumes across adolescence in males and females: A multisample study of longitudinal changes. *NeuroImage* **172**, 194–205 (2018).
24. M. M. Herting, E. R. Sowell, Puberty and structural brain development in humans. *Front. Neuroendocrinol.* **44**, 122–137 (2017).
25. S. Brockmeyer, A. d'Angiulli, How air pollution alters brain development: the role of neuroinflammation. *Transl. Neurosci.* **7**, 24–30 (2016).
26. M. M. Herting, D. Younan, C. E. Campbell, J.-C. Chen, Outdoor Air Pollution and Brain Structure and Function From Across Childhood to Young Adulthood: A Methodological Review of Brain MRI Studies. *Front. Public Health* **7** (2019).
27. Y. Wang, Y. Zhong, J. Liao, G. Wang, PM2.5-related cell death patterns. *Int. J. Med. Sci.* **18**, 1024–1029 (2021).
28. J. L. Allen, C. Klocke, K. Morris-Schaffer, K. Conrad, M. Sobolewski, D. A. Cory-Slechta, Cognitive Effects of Air Pollution Exposures and Potential Mechanistic Underpinnings. *Curr. Environ. Health Rep.* **4**, 180–191 (2017).
29. L. K. Fonken, X. Xu, Z. M. Weil, G. Chen, Q. Sun, S. Rajagopalan, R. J. Nelson, Air pollution impairs cognition, provokes depressive-like behaviors and alters hippocampal cytokine expression and morphology. *Mol. Psychiatry* **16**, 987–995 (2011).
30. N. C. Woodward, A. Haghani, R. G. Johnson, T. M. Hsu, A. Saffari, C. Sioutas, S. E. Kanoski, C. E. Finch, T. E. Morgan, Prenatal and early life exposure to air pollution induced hippocampal vascular leakage and impaired neurogenesis in association with behavioral deficits. *Transl. Psychiatry* **8**, 1–10 (2018).
31. L. Calderón-Garcidueñas, A. Mora-Tiscareño, M. Styner, G. Gómez-garza, H. Zhu, R. Torres-Jardón, E. Carlos, E. Solorio-López, H. Medina-Cortina, M. Kavanaugh, A. D'Angiulli, White Matter Hyperintensities, Systemic Inflammation, Brain Growth, and Cognitive Functions in Children Exposed to Air Pollution. *J. Alzheimers Dis.* **31**, 183–191 (2012).
32. L. Calderón-Garcidueñas, A. C. Solt, C. Henríquez-Roldán, R. Torres-Jardón, B. Nuse, L. Herritt, R. Villarreal-Calderón, N. Osnaya, I. Stone, R. García, D. M. Brooks, A. González-Maciel, R. Reynoso-Robles, R. Delgado-Chávez, W. Reed, Long-term Air Pollution Exposure Is Associated with Neuroinflammation, an Altered Innate Immune Response, Disruption of the Blood-Brain Barrier, Ultrafine Particulate Deposition, and Accumulation of Amyloid β-42 and α-Synuclein in Children and Young Adults. *Toxicol. Pathol.* **36**, 289–310 (2008).
33. L. Calderón-Garcidueñas, R. Reynoso-Robles, J. Vargas-Martínez, A. Gómez-Maqueo-Chew, B. Pérez-Guillé, P. S. Mukherjee, R. Torres-Jardón, G. Perry, A. Gónzalez-Maciel, Prefrontal white matter pathology in air pollution exposed Mexico City young urbanites and their potential impact on neurovascular unit dysfunction and the development of Alzheimer's disease. *Environ. Res.* **146**, 404–417 (2016).
34. L. Calderón-Garcidueñas, A. Calderón-Garcidueñas, R. Torres-Jardón, J. Avila-Ramírez, R. J. Kulesza, A. D. Angiulli, Air pollution and your brain: what do you need to know right now. *Prim. Health Care Res. Dev.* **16**, 329–345 (2015).
35. A.-C. Binter, M. S. W. Kusters, M. A. van den Dries, L. Alonso, M. J. Lubczyńska, G. Hoek, T. White, C. Iñiguez, H. Tiemeier, M. Guxens, Air pollution, white matter microstructure, and brain volumes: Periods

of susceptibility from pregnancy to preadolescence. *Environ. Pollut.* **313**, 120109 (2022).
36. E. Burnor, D. Cserbik, D. L. Cotter, C. E. Palmer, H. Ahmadi, S. P. Eckel, K. Berhane, R. McConnell, J.-C. Chen, J. Schwartz, R. Jackson, M. M. Herting, Association of Outdoor Ambient Fine Particulate Matter With Intracellular White Matter Microstructural Properties Among Children. *JAMA Netw. Open* **4**, e2138300 (2021).
37. M. T. Huuskonen, Q. Liu, K. Lamorie-Foote, K. Shkirkova, M. Connor, A. Patel, A. Montagne, H. Baertsch, C. Sioutas, T. E. Morgan, C. E. Finch, B. V. Zlokovic, W. J. Mack, Air Pollution Particulate Matter Amplifies White Matter Vascular Pathology and Demyelination Caused by Hypoperfusion. *Front. Immunol.* **12**, 785519 (2021).
38. P. de Prado Bert, E. M. H. Mercader, J. Pujol, J. Sunyer, M. Mortamais, The Effects of Air Pollution on the Brain: a Review of Studies Interfacing Environmental Epidemiology and Neuroimaging. *Curr. Environ. Health Rep.* **5**, 351–364 (2018).
39. M. J. Lubczyńska, R. L. Muetzel, H. El Marroun, G. Hoek, I. M. Kooter, E. M. Thomson, M. Hillegers, M. W. Vernooij, T. White, H. Tiemeier, M. Guxens, Air pollution exposure during pregnancy and childhood and brain morphology in preadolescents. *Environ. Res.* **198**, 110446 (2021).
40. B. S. Peterson, R. Bansal, S. Sawardekar, C. Nati, E. R. Elgabalawy, L. A. Hoepner, W. Garcia, X. Hao, A. Margolis, F. Perera, V. Rauh, Prenatal exposure to air pollution is associated with altered brain structure, function, and metabolism in childhood. *J. Child Psychol. Psychiatry* **63**, 1316–1331 (2022).
41. K. Sukumaran, C. Cardenas-Iniguez, E. Burnor, K. L. Bottenhorn, D. A. Hackman, R. McConnell, K. Berhane, J. Schwartz, J.-C. Chen, M. M. Herting, Ambient fine particulate exposure and subcortical gray matter microarchitecture in 9- and 10-year-old children across the United States. *iScience* **26**, 106087 (2023).
42. N. S. White, T. B. Leergaard, H. D'Arceuil, J. G. Bjaalie, A. M. Dale, Probing tissue microstructure with restriction spectrum imaging: Histological and theoretical validation. *Hum. Brain Mapp.* **34**, 327–346 (2012).
43. C. E. Palmer, D. Pecheva, J. R. Iversen, D. J. Hagler, L. Sugrue, P. Nedelec, C. C. Fan, W. K. Thompson, T. L. Jernigan, A. M. Dale, Microstructural development from 9 to 14 years: Evidence from the ABCD Study. *Dev. Cogn. Neurosci.* **53**, 101044 (2022).
44. K. L. Bottenhorn, C. Cardenas-Iniguez, K. L. Mills, A. R. Laird, M. M. Herting, Profiling intra- and inter-individual differences in brain development across early adolescence. *NeuroImage* **279**, 120287 (2023).
45. R. A. Carper, J. M. Treiber, N. S. White, J. S. Kohli, R.-A. Müller, Restriction Spectrum Imaging As a Potential Measure of Cortical Neurite Density in Autism. *Front. Neurosci.* **10** (2017).
46. M. I. Conley, L. J. Skalaban, K. M. Rapuano, R. Gonzalez, A. R. Laird, A. S. Dick, M. T. Sutherland, R. Watts, B. J. Casey, Altered hippocampal microstructure and function in children who experienced Hurricane Irma. *Dev. Psychobiol.* **63**, 864–877 (2021).
47. B. T. Newman, J. T. Patrie, T. J. Druzgal, An intracellular isotropic diffusion signal is positively associated with pubertal development in white matter. *Dev. Cogn. Neurosci.* **63**, 101301 (2023).
48. K. M. Rapuano, J. S. Laurent, D. J. Hagler, S. N. Hatton, W. K. Thompson, T. L. Jernigan, A. M. Dale, B. J. Casey, R. Watts, Nucleus accumbens cytoarchitecture predicts weight gain in children. *Proc. Natl. Acad. Sci.* **117**, 26977–26984 (2020).
49. H. Garavan, H. Bartsch, K. Conway, A. Decastro, R. Z. Goldstein, S. Heeringa, T. Jernigan, A. Potter, W. Thompson, D. Zahs, Recruiting the ABCD sample: Design considerations and procedures. *Dev. Cogn. Neurosci.* **32**, 16–22 (2018).
50. N. D. Volkow, G. F. Koob, R. T. Croyle, D. W. Bianchi, J. A. Gordon, W. J. Koroshetz, E. J. Pérez-Stable, W. T. Riley, M. H. Bloch, K. Conway, B. G. Deeds, G. J. Dowling, S. Grant, K. D. Howlett, J. A. Matochik, G. D. Morgan, M. M. Murray, A. Noronha, C. Y. Spong, E. M. Wargo, K. R. Warren, S. R. B. Weiss, The conception of the ABCD study: From substance use to a broad NIH collaboration. *Dev. Cogn. Neurosci.* **32**, 4–7 (2018).
51. D. J. Hagler, S. Hatton, M. D. Cornejo, C. Makowski, D. A. Fair, A. S. Dick, M. T. Sutherland, B. J. Casey, D. M. Barch, M. P. Harms, R. Watts, J. M. Bjork, H. P. Garavan, L. Hilmer, C. J. Pung, C. S. Sicat, J. Kuperman, H. Bartsch, F. Xue, M. M. Heitzeg, A. R. Laird, T. T. Trinh, R. Gonzalez, S. F. Tapert, M. C. Riedel, L. M. Squeglia, L. W. Hyde, M. D. Rosenberg, E. A. Earl, K. D. Howlett, F. C. Baker, M. Soules, J. Diaz, O. R. de Leon, W. K. Thompson, M. C. Neale, M. Herting, E. R. Sowell, R. P. Alvarez, S. W. Hawes, M. Sanchez, J. Bodurka, F. J. Breslin, A. S. Morris, M. P. Paulus, W. K. Simmons, J. R. Polimeni, A. van der Kouwe, A. S. Nencka, K. M. Gray, C. Pierpaoli, J. A. Matochik, A. Noronha, W. M. Aklin, K. Conway, M. Glantz, E. Hoffman, R. Little, M. Lopez, V. Pariyadath, S. R. Weiss, D. L. Wolff-Hughes, R. DelCarmen-Wiggins, S. W. Feldstein Ewing, O. Miranda-Dominguez, B. J. Nagel, A. J. Perrone, D. T. Sturgeon, A. Goldstone, A. Pfefferbaum, K. M. Pohl, D. Prouty, K. Uban, S. Y. Bookheimer, M. Dapretto, A. Galvan, K. Bagot, J. Giedd,

M. A. Infante, J. Jacobus, K. Patrick, P. D. Shilling, R. Desikan, Y. Li, L. Sugrue, M. T. Banich, N. Friedman, J. K. Hewitt, C. Hopfer, J. Sakai, J. Tanabe, L. B. Cottler, S. J. Nixon, L. Chang, C. Cloak, T. Ernst, G. Reeves, D. N. Kennedy, S. Heeringa, S. Peltier, J. Schulenberg, C. Sripada, R. A. Zucker, W. G. Iacono, M. Luciana, F. J. Calabro, D. B. Clark, D. A. Lewis, B. Luna, C. Schirda, T. Brima, J. J. Foxe, E. G. Freedman, D. W. Mruzek, M. J. Mason, R. Huber, E. McGlade, A. Prescot, P. F. Renshaw, D. A. Yurgelun-Todd, N. A. Allgaier, J. A. Dumas, M. Ivanova, A. Potter, P. Florsheim, C. Larson, K. Lisdahl, M. E. Charness, B. Fuemmeler, J. M. Hettema, H. H. Maes, J. Steinberg, A. P. Anokhin, P. Glaser, A. C. Heath, P. A. Madden, A. Baskin-Sommers, R. T. Constable, S. J. Grant, G. J. Dowling, S. A. Brown, T. L. Jernigan, A. M. Dale, Image processing and analysis methods for the Adolescent Brain Cognitive Development Study. *NeuroImage* **202**, 116091 (2019).

52. S. G. Heeringa, P. A. Berglund, "A Guide for Population-based Analysis of the Adolescent Brain Cognitive Development (ABCD) Study Baseline Data" (preprint, Neuroscience, 2020); https://doi.org/10.1101/2020.02.10.942011.
53. R. C. Oldfield, The assessment and analysis of handedness: the Edinburgh inventory. *Neuropsychologia* **9**, 97–113 (1971).
54. J. F. Veale, Edinburgh handedness inventory–short form: a revised version based on confirmatory factor analysis. *Laterality Asymmetries Body Brain Cogn.* **19**, 164–177 (2014).
55. M. P. Paulus, L. M. Squeglia, K. Bagot, J. Jacobus, R. Kuplicki, F. J. Breslin, J. Bodurka, A. S. Morris, W. K. Thompson, H. Bartsch, S. F. Tapert, Screen media activity and brain structure in youth: Evidence for diverse structural correlation networks from the ABCD study. *NeuroImage* **185**, 140–153 (2019).
56. K. N. Paulich, J. M. Ross, J. M. Lessem, J. K. Hewitt, Screen time and early adolescent mental health, academic, and social outcomes in 9- and 10- year old children: Utilizing the Adolescent Brain Cognitive Development [SM] (ABCD) Study. *PloS One* **16**, e0256591 (2021).
57. D. M. Barch, M. D. Albaugh, S. Avenevoli, L. Chang, D. B. Clark, M. D. Glantz, J. J. Hudziak, T. L. Jernigan, S. F. Tapert, D. Yurgelun-Todd, N. Alia-Klein, A. S. Potter, M. P. Paulus, D. Prouty, R. A. Zucker, K. J. Sher, Demographic, physical and mental health assessments in the adolescent brain and cognitive development study: Rationale and description. *Dev. Cogn. Neurosci.* **32**, 55–66 (2018).
58. S. E. Echeverria, A. V. Diez-Roux, B. G. Link, Reliability of self-reported neighborhood characteristics. *J. Urban Health Bull. N. Y. Acad. Med.* **81**, 682–701 (2004).
59. M. S. Mujahid, A. V. Diez Roux, J. D. Morenoff, T. Raghunathan, Assessing the measurement properties of neighborhood scales: from psychometrics to ecometrics. *Am. J. Epidemiol.* **165**, 858–867 (2007).
60. C. C. Fan, A. Marshall, H. Smolker, M. R. Gonzalez, S. F. Tapert, D. M. Barch, E. Sowell, G. J. Dowling, C. Cardenas-Iniguez, J. Ross, W. K. Thompson, M. M. Herting, Adolescent Brain Cognitive Development (ABCD) study Linked External Data (LED): Protocol and practices for geocoding and assignment of environmental data. *Dev. Cogn. Neurosci.* **52**, 101030 (2021).
61. Center for International Earth Science Information Network. http://www.ciesin.org/data.html.
62. D. Mennitt, K. Sherrill, K. Fristrup, A geospatial model of ambient sound pressure levels in the contiguous United States. *J. Acoust. Soc. Am.* **135**, 2746–2764 (2014).
63. B. J. Casey, T. Cannonier, M. I. Conley, A. O. Cohen, D. M. Barch, M. M. Heitzeg, M. E. Soules, T. Teslovich, D. Dellarco, H. Garavan, C. A. Orr, T. D. Wager, M. T. Banich, N. K. Speer, M. T. Sutherland, M. C. Riedel, A. S. Dick, J. M. Bjork, K. M. Thomas, B. Chaarani, M. H. Mejia, D. J. Hagler, M. Daniela Cornejo, C. S. Sicat, M. P. Harms, N. U. F. Dosenbach, M. Rosenberg, E. Earl, H. Bartsch, R. Watts, J. R. Polimeni, J. M. Kuperman, D. A. Fair, A. M. Dale, The Adolescent Brain Cognitive Development (ABCD) study: Imaging acquisition across 21 sites. *Dev. Cogn. Neurosci.* **32**, 43–54 (2018).
64. L. S. Gorham, D. M. Barch, White Matter Tract Integrity, Involvement in Sports, and Depressive Symptoms in Children. *Child Psychiatry Hum. Dev.* **51**, 490–501 (2020).
65. N. S. White, C. McDonald, N. Farid, J. Kuperman, D. Karow, N. M. Schenker-Ahmed, H. Bartsch, R. Rakow-Penner, D. Holland, A. Shabaik, A. Bjørnerud, T. Hope, J. Hattangadi-Gluth, M. Liss, J. K. Parsons, C. C. Chen, S. Raman, D. Margolis, R. E. Reiter, L. Marks, S. Kesari, A. J. Mundt, C. J. Kane, B. S. Carter, W. G. Bradley, A. M. Dale, Diffusion-weighted imaging in cancer: Physical foundations and applications of Restriction Spectrum Imaging. *Cancer Res.* **74**, 4638–4652 (2014).
66. N. S. White, C. R. McDonald, N. Farid, J. M. Kuperman, S. Kesari, A. M. Dale, Improved Conspicuity and Delineation of High-Grade Primary and Metastatic Brain Tumors Using "Restriction Spectrum Imaging": Quantitative Comparison with High B-Value DWI and ADC. *Am. J. Neuroradiol.* **34**, 958–964 (2013).
67. R. S. Desikan, F. Ségonne, B. Fischl, B. T. Quinn, B. C. Dickerson, D. Blacker, R. L. Buckner, A. M. Dale, R. P.

Maguire, B. T. Hyman, M. S. Albert, R. J. Killiany, An automated labeling system for subdividing the human cerebral cortex on MRI scans into gyral based regions of interest. *NeuroImage* **31**, 968–980 (2006).
68. Q. Di, H. Amini, L. Shi, I. Kloog, R. Silvern, J. Kelly, M. B. Sabath, C. Choirat, P. Koutrakis, A. Lyapustin, An ensemble-based model of PM2. 5 concentration across the contiguous United States with high spatiotemporal resolution. *Environ. Int.* **130**, 104909 (2019).
69. Q. Di, H. Amini, L. Shi, I. Kloog, R. Silvern, J. Kelly, M. B. Sabath, C. Choirat, P. Koutrakis, A. Lyapustin, Y. Wang, L. J. Mickley, J. Schwartz, Assessing NO2 Concentration and Model Uncertainty with High Spatiotemporal Resolution across the Contiguous United States Using Ensemble Model Averaging. *Environ. Sci. Technol.* **54**, 1372–1384 (2020).
70. H. Amini, M. Danesh-Yazdi, W. Requia, Y. Wei, Y. Abu-Awad, L. Shi, M. Franklin, C.-M. Kang, J. Wolfson, P. James, R. Habre, Q. Zhu, J. Apte, Z. Andersen, I. Kloog, F. Dominici, P. Koutrakis, J. Schwartz, Hyperlocal super-learned PM2.5 components across the contiguous US. Research Square [Preprint] (2022). https://doi.org/10.21203/rs.3.rs-1745433/v1.
71. T. Jin, H. Amini, A. Kosheleva, M. Danesh Yazdi, Y. Wei, E. Castro, Q. Di, L. Shi, J. Schwartz, Associations between long-term exposures to airborne PM2.5 components and mortality in Massachusetts: mixture analysis exploration. *Environ. Health* **21**, 96 (2022).
72. A. Krishnan, L. J. Williams, A. R. McIntosh, H. Abdi, Partial Least Squares (PLS) methods for neuroimaging: A tutorial and review. *NeuroImage* **56**, 455–475 (2011).
73. A. R. McIntosh, N. J. Lobaugh, Partial least squares analysis of neuroimaging data: applications and advances. *NeuroImage* **23**, S250–S263 (2004).
74. D. Beaton, C. R. Chin Fatt, H. Abdi, An ExPosition of multivariate analysis with the singular value decomposition in R. *Comput. Stat. Data Anal.* **72**, 176–189 (2014).
75. H. Abdi, D. Beaton, *Principal Component and Correspondence Analyses Using R* (Springer Cham, 2023; https://link.springer.com/book/9783319092577)*SpringerBriefs in Statistics*.
76. H. Abdi, L. J. Williams, Partial least squares methods: partial least squares correlation and partial least square regression. *Comput. Toxicol. Vol. II*, 549–579 (2013).
77. V. Menon, Large-scale brain networks and psychopathology: a unifying triple network model. *Trends Cogn. Sci.* **15**, 483–506 (2011).
78. M. J. Lubczyńska, R. L. Muetzel, H. El Marroun, X. Basagaña, M. Strak, W. Denault, V. W. V. Jaddoe, M. Hillegers, M. W. Vernooij, G. Hoek, T. White, B. Brunekreef, H. Tiemeier, M. Guxens, Exposure to Air Pollution during Pregnancy and Childhood, and White Matter Microstructure in Preadolescents. *Environ. Health Perspect.* **128**, 027005 (2020).
79. B. S. Peterson, V. A. Rauh, R. Bansal, X. Hao, Z. Toth, G. Nati, K. Walsh, R. L. Miller, F. Arias, D. Semanek, F. Perera, Effects of Prenatal Exposure to Air Pollutants (Polycyclic Aromatic Hydrocarbons) on the Development of Brain White Matter, Cognition, and Behavior in Later Childhood. *JAMA Psychiatry* **72**, 531–540 (2015).
80. K. L. Mills, K. D. Siegmund, C. K. Tamnes, L. Ferschmann, L. M. Wierenga, M. G. N. Bos, B. Luna, C. Li, M. M. Herting, Inter-individual variability in structural brain development from late childhood to young adulthood. *NeuroImage* **242**, 118450 (2021).
81. C. Aoki, R. D. Romeo, S. S. Smith, Adolescence as a critical period for developmental plasticity. *Brain Res.* **1654**, 85–86 (2017).
82. S. M. Schalbetter, A. S. von Arx, N. Cruz-Ochoa, K. Dawson, A. Ivanov, F. S. Mueller, H.-Y. Lin, R. Amport, W. Mildenberger, D. Mattei, D. Beule, C. Földy, M. Greter, T. Notter, U. Meyer, Adolescence is a sensitive period for prefrontal microglia to act on cognitive development. *Sci. Adv.* **8**, eabi6672 (2022).
83. I. Opris, M. F. Casanova, Prefrontal cortical minicolumn: from executive control to disrupted cognitive processing. *Brain* **137**, 1863–1875 (2014).
84. P. R. Huttenlocher, A. S. Dabholkar, Regional differences in synaptogenesis in human cerebral cortex. *J. Comp. Neurol.* **387**, 167–178 (1997).
85. L. D. Selemon, A role for synaptic plasticity in the adolescent development of executive function. *Transl. Psychiatry* **3**, e238–e238 (2013).
86. S. Brot, V. Rogemond, V. Perrot, N. Chounlamountri, C. Auger, J. Honnorat, M. Moradi-Améli, CRMP5 Interacts with Tubulin to Inhibit Neurite Outgrowth, Thereby Modulating the Function of CRMP2. *J. Neurosci.* **30**, 10639–10654 (2010).
87. C. C. Fan, R. Loughnan, C. Makowski, D. Pecheva, C.-H. Chen, D. J. Hagler, W. K. Thompson, N. Parker, D. van der Meer, O. Frei, O. A. Andreassen, A. M. Dale, Multivariate genome-wide association study on

tissue-sensitive diffusion metrics highlights pathways that shape the human brain. *Nat. Commun.* **13**, 2423 (2022).
88. D. Vidal-Pineiro, N. Parker, J. Shin, L. French, H. Grydeland, A. P. Jackowski, A. M. Mowinckel, Y. Patel, Z. Pausova, G. Salum, Ø. Sørensen, K. B. Walhovd, T. Paus, A. M. Fjell, Cellular correlates of cortical thinning throughout the lifespan. *Sci. Rep.* **10**, 21803 (2020).
89. P. Gillespie, J. Tajuba, M. Lippmann, L.-C. Chen, B. Veronesi, Particulate matter neurotoxicity in culture is size-dependent. *NeuroToxicology* **36**, 112–117 (2013).
90. L. E. Clarke, S. A. Liddelow, C. Chakraborty, A. E. Münch, M. Heiman, B. A. Barres, Normal aging induces A1-like astrocyte reactivity. *Proc. Natl. Acad. Sci.* **115**, E1896–E1905 (2018).
91. M. Olah, E. Patrick, A.-C. Villani, J. Xu, C. C. White, K. J. Ryan, P. Piehowski, A. Kapasi, P. Nejad, M. Cimpean, S. Connor, C. J. Yung, M. Frangieh, A. McHenry, W. Elyaman, V. Petyuk, J. A. Schneider, D. A. Bennett, P. L. De Jager, E. M. Bradshaw, A transcriptomic atlas of aged human microglia. *Nat. Commun.* **9**, 539 (2018).
92. L. Calderón-Garcidueñas, A. Gónzalez-Maciel, R. Reynoso-Robles, R. Delgado-Chávez, P. S. Mukherjee, R. J. Kulesza, R. Torres-Jardón, J. Ávila-Ramírez, R. Villarreal-Ríos, Hallmarks of Alzheimer disease are evolving relentlessly in Metropolitan Mexico City infants, children and young adults. APOE4 carriers have higher suicide risk and higher odds of reaching NFT stage V at ≤ 40 years of age. *Environ. Res.* **164**, 475–487 (2018).
93. L. Calderón-Garcidueñas, R. Torres-Jardón, R. J. Kulesza, Y. Mansour, L. O. González-González, A. Gónzalez-Maciel, R. Reynoso-Robles, P. S. Mukherjee, Alzheimer disease starts in childhood in polluted Metropolitan Mexico City. A major health crisis in progress. *Environ. Res.* **183**, 109137 (2020).
94. S.-H. Lee, Y.-H. Chen, C.-C. Chien, Y.-H. Yan, H.-C. Chen, H.-C. Chuang, H.-I. Hsieh, K.-H. Cho, L.-W. Kuo, C. C.-K. Chou, M.-J. Chiu, B. L. Tee, T.-F. Chen, T.-J. Cheng, Three month inhalation exposure to low-level PM2.5 induced brain toxicity in an Alzheimer's disease mouse model. *PLOS ONE* **16**, e0254587 (2021).
95. D. P. Bhatt, K. L. Puig, M. W. Gorr, L. E. Wold, C. K. Combs, A Pilot Study to Assess Effects of Long-Term Inhalation of Airborne Particulate Matter on Early Alzheimer-Like Changes in the Mouse Brain. *PLOS ONE* **10**, e0127102 (2015).
96. Y. Shou, X. Zhu, D. Zhu, H. Yin, Y. Shi, M. Chen, L. Lu, Q. Qian, D. Zhao, Y. Hu, H. Wang, Ambient PM2.5 chronic exposure leads to cognitive decline in mice: From pulmonary to neuronal inflammation. *Toxicol. Lett.* **331**, 208–217 (2020).
97. L. Calderón-Garcidueñas, R. Engle, A. Mora-Tiscareño, M. Styner, G. Gómez-Garza, H. Zhu, V. Jewells, R. Torres-Jardón, L. Romero, M. E. Monroy-Acosta, C. Bryant, L. O. González-González, H. Medina-Cortina, A. D'Angiulli, Exposure to severe urban air pollution influences cognitive outcomes, brain volume and systemic inflammation in clinically healthy children. *Brain Cogn.* **77**, 345–355 (2011).
98. L. Calderón-Garcidueñas, R. Torres-Jardón, R. J. Kulesza, S.-B. Park, A. D'Angiulli, Air pollution and detrimental effects on children's brain. The need for a multidisciplinary approach to the issue complexity and challenges. *Front. Hum. Neurosci.* **8** (2014).
99. K.-H. Tse, K. Herrup, Re-imagining Alzheimer's disease – the diminishing importance of amyloid and a glimpse of what lies ahead. *J. Neurochem.* **143**, 432–444 (2017).
100. G. Di Benedetto, C. Burgaletto, C. M. Bellanca, A. Munafò, R. Bernardini, G. Cantarella, Role of Microglia and Astrocytes in Alzheimer's Disease: From Neuroinflammation to Ca2+ Homeostasis Dysregulation. *Cells* **11**, 2728 (2022).
101. P. Fu, X. Guo, F. M. H. Cheung, K. K. L. Yung, The association between PM2.5 exposure and neurological disorders: A systematic review and meta-analysis. *Sci. Total Environ.* **655**, 1240–1248 (2019).
102. S. H. Rhew, J. Kravchenko, H. K. Lyerly, Exposure to low-dose ambient fine particulate matter PM2.5 and Alzheimer's disease, non-Alzheimer's dementia, and Parkinson's disease in North Carolina. *PLOS ONE* **16**, e0253253 (2021).
103. Y. Shou, Y. Huang, X. Zhu, C. Liu, Y. Hu, H. Wang, A review of the possible associations between ambient PM2.5 exposures and the development of Alzheimer's disease. *Ecotoxicol. Environ. Saf.* **174**, 344–352 (2019).
104. K. Thiankhaw, N. Chattipakorn, S. C. Chattipakorn, PM2.5 exposure in association with AD-related neuropathology and cognitive outcomes. *Environ. Pollut. Barking Essex 1987* **292**, 118320 (2022).
105. J. Li, Y. Wang, K. Steenland, P. Liu, A. van Donkelaar, R. V. Martin, H. H. Chang, W. M. Caudle, J. Schwartz, P. Koutrakis, L. Shi, Long-term effects of PM2.5 components on incident dementia in the northeastern United States. *The Innovation* **3** (2022).

106. R. B. Bernardi, A. C. T. Zanchi, N. R. Damaceno-Rodrigues, M. M. Veras, P. H. N. Saldiva, H. M. T. Barros, C. R. Rhoden, The impact of chronic exposure to air pollution over oxidative stress parameters and brain histology. *Environ. Sci. Pollut. Res.* **28**, 47407–47417 (2021).
107. D. Cserbik, J.-C. Chen, R. McConnell, K. Berhane, E. R. Sowell, J. Schwartz, D. A. Hackman, E. Kan, C. C. Fan, M. M. Herting, Fine particulate matter exposure during childhood relates to hemispheric-specific differences in brain structure. *Environ. Int.* **143**, 105933 (2020).
108. B. C. Nephew, A. Nemeth, N. Hudda, G. Beamer, P. Mann, J. Petitto, R. Cali, M. Febo, P. Kulkarni, G. Poirier, J. King, J. L. Durant, D. Brugge, Traffic-related particulate matter affects behavior, inflammation, and neural integrity in a developmental rodent model. *Environ. Res.* **183**, 109242 (2020).
109. M. G. Adam, P. T. M. Tran, N. Bolan, R. Balasubramanian, Biomass burning-derived airborne particulate matter in Southeast Asia: A critical review. *J. Hazard. Mater.* **407**, 124760 (2021).
110. H. J. Johnston, W. Mueller, S. Steinle, S. Vardoulakis, K. Tantrakarnapa, M. Loh, J. W. Cherrie, How Harmful Is Particulate Matter Emitted from Biomass Burning? A Thailand Perspective. *Curr. Pollut. Rep.* **5**, 353–377 (2019).
111. H. Z. Li, T. R. Dallmann, X. Li, P. Gu, A. A. Presto, Urban Organic Aerosol Exposure: Spatial Variations in Composition and Source Impacts. *Environ. Sci. Technol.* **52**, 415–426 (2018).
112. K. M. Robinson, J. A. B. Price, B. Demyen, Understanding arithmetic concepts: Does operation matter? *J. Exp. Child Psychol.* **166**, 421–436 (2018).
113. C. E. Stockwell, P. R. Veres, J. Williams, R. J. Yokelson, Characterization of biomass burning emissions from cooking fires, peat, crop residue, and other fuels with high-resolution proton-transfer-reaction time-of-flight mass spectrometry. *Atmospheric Chem. Phys.* **15**, 845–865 (2015).
114. M. M. Rahman, G. Thurston, A hybrid satellite and land use regression model of source-specific PM2.5 and PM2.5 constituents. *Environ. Int.* **163**, 107233 (2022).
115. J. R. Krall, J. A. Mulholland, A. G. Russell, S. Balachandran, A. Winquist, P. E. Tolbert, L. A. Waller, S. E. Sarnat, Associations between Source-Specific Fine Particulate Matter and Emergency Department Visits for Respiratory Disease in Four U.S. Cities. *Environ. Health Perspect.* **125**, 97–103 (2017).
116. B. Ostro, W.-Y. Feng, R. Broadwin, S. Green, M. Lipsett, The Effects of Components of Fine Particulate Air Pollution on Mortality in California: Results from CALFINE. *Environ. Health Perspect.* **115**, 13–19 (2007).
117. J. Chen, G. Hoek, K. de Hoogh, S. Rodopoulou, Z. J. Andersen, T. Bellander, J. Brandt, D. Fecht, F. Forastiere, J. Gulliver, O. Hertel, B. Hoffmann, U. A. Hvidtfeldt, W. M. M. Verschuren, K.-H. Jöckel, J. T. Jørgensen, K. Katsouyanni, M. Ketzel, D. Y. Méndez, K. Leander, S. Liu, P. Ljungman, E. Faure, P. K. E. Magnusson, G. Nagel, G. Pershagen, A. Peters, O. Raaschou-Nielsen, D. Rizzuto, E. Samoli, Y. T. van der Schouw, S. Schramm, G. Severi, M. Stafoggia, M. Strak, M. Sørensen, A. Tjønneland, G. Weinmayr, K. Wolf, E. Zitt, B. Brunekreef, G. D. Thurston, Long-Term Exposure to Source-Specific Fine Particles and Mortality—A Pooled Analysis of 14 European Cohorts within the ELAPSE Project. *Environ. Sci. Technol.* **56**, 9277–9290 (2022).
118. K. Huttunen, T. Siponen, I. Salonen, T. Yli-Tuomi, M. Aurela, H. Dufva, R. Hillamo, E. Linkola, J. Pekkanen, A. Pennanen, A. Peters, R. O. Salonen, A. Schneider, P. Tiittanen, M.-R. Hirvonen, T. Lanki, Low-level exposure to ambient particulate matter is associated with systemic inflammation in ischemic heart disease patients. *Environ. Res.* **116**, 44–51 (2012).
119. T. Siponen, T. Yli-Tuomi, M. Aurela, H. Dufva, R. Hillamo, M.-R. Hirvonen, K. Huttunen, J. Pekkanen, A. Pennanen, I. Salonen, P. Tiittanen, R. O. Salonen, T. Lanki, Source-specific fine particulate air pollution and systemic inflammation in ischaemic heart disease patients. *Occup. Environ. Med.* **72**, 277–283 (2015).
120. S. Achilleos, M.-A. Kioumourtzoglou, C.-D. Wu, J. D. Schwartz, P. Koutrakis, S. I. Papatheodorou, Acute effects of fine particulate matter constituents on mortality: A systematic review and meta-regression analysis. *Environ. Int.* **109**, 89–100 (2017).
121. C. E. Reid, M. Brauer, F. H. Johnston, M. Jerrett, J. R. Balmes, C. T. Elliott, Critical Review of Health Impacts of Wildfire Smoke Exposure. *Environ. Health Perspect.* **124**, 1334–1343 (2016).
122. M. Jankowska-Kieltyka, A. Roman, I. Nalepa, The Air We Breathe: Air Pollution as a Prevalent Proinflammatory Stimulus Contributing to Neurodegeneration. *Front. Cell. Neurosci.* **15** (2021).
123. L. A. Milton, A. R. White, The potential impact of bushfire smoke on brain health. *Neurochem. Int.* **139**, 104796 (2020).
124. R. You, Y.-S. Ho, R. C.-C. Chang, The pathogenic effects of particulate matter on neurodegeneration: a review. *J. Biomed. Sci.* **29**, 15 (2022).
125. B. A. Maher, I. A. M. Ahmed, V. Karloukovski, D. A. MacLaren, P. G. Foulds, D. Allsop, D. M. A. Mann, R.

Torres-Jardón, L. Calderon-Garciduenas, Magnetite pollution nanoparticles in the human brain. *Proc. Natl. Acad. Sci.* **113**, 10797–10801 (2016).
126. L. Calderón-Garcidueñas, M. Franco-Lira, C. Henríquez-Roldán, N. Osnaya, A. González-Maciel, R. Reynoso-Robles, R. Villarreal-Calderon, L. Herritt, D. Brooks, S. Keefe, Urban air pollution: influences on olfactory function and pathology in exposed children and young adults. *Exp. Toxicol. Pathol.* **62**, 91–102 (2010).
127. A. Campbell, M. Oldham, A. Becaria, S. C. Bondy, D. Meacher, C. Sioutas, C. Misra, L. B. Mendez, M. Kleinman, Particulate matter in polluted air may increase biomarkers of inflammation in mouse brain. *Neurotoxicology* **26**, 133–140 (2005).
128. L. S. Fagundes, A. da S. Fleck, A. C. Zanchi, P. H. N. Saldiva, C. R. Rhoden, Direct contact with particulate matter increases oxidative stress in different brain structures. *Inhal. Toxicol.* **27**, 462–467 (2015).
129. D. Scieszka, R. Hunter, J. Begay, M. Bitsui, Y. Lin, J. Galewsky, M. Morishita, Z. Klaver, J. Wagner, J. R. Harkema, G. Herbert, S. Lucas, C. McVeigh, A. Bolt, B. Bleske, C. G. Canal, E. Mostovenko, A. K. Ottens, H. Gu, M. J. Campen, S. Noor, Neuroinflammatory and Neurometabolomic Consequences From Inhaled Wildfire Smoke-Derived Particulate Matter in the Western United States. *Toxicol. Sci. Off. J. Soc. Toxicol.* **186**, 149–162 (2022).
130. N. C. Woodward, M. C. Levine, A. Haghani, F. Shirmohammadi, A. Saffari, C. Sioutas, T. E. Morgan, C. E. Finch, Toll-like receptor 4 in glial inflammatory responses to air pollution in vitro and in vivo. *J. Neuroinflammation* **14**, 1–15 (2017).
131. Q. Zhang, Q. Li, J. Ma, Y. Zhao, PM2. 5 impairs neurobehavior by oxidative stress and myelin sheaths injury of brain in the rat. *Environ. Pollut.* **242**, 994–1001 (2018).
132. M. E. Gerlofs-Nijland, D. van Berlo, F. R. Cassee, R. P. Schins, K. Wang, A. Campbell, Effect of prolonged exposure to diesel engine exhaust on proinflammatory markers in different regions of the rat brain. *Part. Fibre Toxicol.* **7**, 1–10 (2010).
133. C. G. Zundel, P. Ryan, C. Brokamp, A. Heeter, Y. Huang, J. R. Strawn, H. A. Marusak, Air pollution, depressive and anxiety disorders, and brain effects: A systematic review. *NeuroToxicology* **93**, 272–300 (2022).
134. V. Planche, J. V. Manjon, B. Mansencal, E. Lanuza, T. Tourdias, G. Catheline, P. Coupé, Structural progression of Alzheimer's disease over decades: the MRI staging scheme. *Brain Commun.* **4**, fcac109 (2022).
135. M. Solmi, J. Radua, M. Olivola, E. Croce, L. Soardo, G. Salazar de Pablo, J. Il Shin, J. B. Kirkbride, P. Jones, J. H. Kim, J. Y. Kim, A. F. Carvalho, M. V. Seeman, C. U. Correll, P. Fusar-Poli, Age at onset of mental disorders worldwide: large-scale meta-analysis of 192 epidemiological studies. *Mol. Psychiatry* **27**, 281–295 (2022).
136. I. Bakolis, R. Hammoud, R. Stewart, S. Beevers, D. Dajnak, S. MacCrimmon, M. Broadbent, M. Pritchard, N. Shiode, D. Fecht, J. Gulliver, M. Hotopf, S. L. Hatch, I. S. Mudway, Mental health consequences of urban air pollution: prospective population-based longitudinal survey. *Soc. Psychiatry Psychiatr. Epidemiol.* **56**, 1587–1599 (2021).
137. J. D. King, S. Zhang, A. Cohen, Air pollution and mental health: associations, mechanisms and methods. *Curr. Opin. Psychiatry* **35**, 192–199 (2022).
138. C. Xie, S. Xiang, C. Shen, X. Peng, J. Kang, Y. Li, W. Cheng, S. He, T. Banaschewski, G. J. Barker, A. L. W. Bokde, U. Bromberg, C. Büchel, S. Desrivières, H. Flor, A. Grigis, H. Garavan, P. Gowland, A. Heinz, B. Ittermann, J.-L. Martinot, M.-L. P. Martinot, F. Nees, D. P. Orfanos, T. Paus, L. Poustka, J. H. Fröhner, M. N. Smolka, H. Walter, R. Whelan, B. J. Sahakian, T. W. Robbins, G. Schumann, T. Jia, J. Feng, A shared neural basis underlying psychiatric comorbidity. *Nat. Med.* **29**, 1232–1242 (2023).
139. C. E. Campbell, D. L. Cotter, K. L. Bottenhorn, E. Burnor, H. Ahmadi, W. J. Gauderman, C. Cardenas-Iniguez, D. Hackman, R. McConnell, K. Berhane, J. Schwartz, J.-C. Chen, M. M. Herting, Air pollution and emotional behavior in adolescents across the U.S. *Environ. Res.*, doi: 10.1101/2023.04.19.23288834 (accepted).
140. C. Milando, L. Huang, S. Batterman, Trends in PM2.5 emissions, concentrations and apportionments in Detroit and Chicago. *Atmospheric Environ. Oxf. Engl. 1994* **129**, 197–209 (2016).
141. S. Singh, G. Johnson, D. W. DuBois, I. G. Kavouras, Assessment of the Contribution of Local and Regional Biomass Burning on PM2.5 in New York/New Jersey Metropolitan Area. *Aerosol Air Qual. Res.* **22**, 220121 (2022).
142. M. Burke, M. L. Childs, B. de la Cuesta, M. Qiu, J. Li, C. F. Gould, S. Heft-Neal, M. Wara, The contribution

of wildfire to PM2.5 trends in the USA. *Nature*, 1–6 (2023).
143. F. Enayati Ahangar, P. Pakbin, S. Hasheminassab, S. A. Epstein, X. Li, A. Polidori, J. Low, Long-term trends of PM2.5 and its carbon content in the South Coast Air Basin: A focus on the impact of wildfires. *Atmos. Environ.* **255**, 118431 (2021).
144. Y. Li, D. Tong, S. Ma, X. Zhang, S. Kondragunta, F. Li, R. Saylor, Dominance of Wildfires Impact on Air Quality Exceedances During the 2020 Record-Breaking Wildfire Season in the United States. *Geophys. Res. Lett.* **48**, e2021GL094908 (2021).
145. K. O'Dell, B. Ford, E. V. Fischer, J. R. Pierce, Contribution of Wildland-Fire Smoke to US PM2.5 and Its Influence on Recent Trends. *Environ. Sci. Technol.* **53**, 1797–1804 (2019).
146. N. Boegelsack, J. Withey, G. O'Sullivan, D. McMartin, A Critical Examination of the Relationship between Wildfires and Climate Change with Consideration of the Human Impact. *J. Environ. Prot.* **9**, 461–467 (2018).
147. S. Deguen, M. Amuzu, V. Simoncic, W. Kihal-Talantikite, Exposome and Social Vulnerability: An Overview of the Literature Review. *Int. J. Environ. Res. Public. Health* **19**, 3534 (2022).
148. A. L. Pearson, E. A. Shewark, S. A. Burt, Associations between neighborhood built, social, or toxicant conditions and child externalizing behaviors in the Detroit metro area: a cross-sectional study of the neighborhood 'exposome.' *BMC Public Health* **22**, 1064 (2022).
149. P. Vineis, What Is the Exposome and How It Can Help Research on Air Pollution. *Emiss. Control Sci. Technol.* **5**, 31–36 (2019).
150. T. W. Collins, S. E. Grineski, Y. Shaker, C. J. Mullen, Communities of color are disproportionately exposed to long-term and short-term PM2.5 in metropolitan America. *Environ. Res.* **214**, 114038 (2022).
151. J. Colmer, I. Hardman, J. Shimshack, J. Voorheis, Disparities in PM2.5 air pollution in the United States. *Science* **369**, 575–578 (2020).